

This is a repository copy of *Holocene mangrove dynamics and relative sea-level changes along the Tanzanian coast, East Africa*.

White Rose Research Online URL for this paper:

<https://eprints.whiterose.ac.uk/136117/>

Version: Accepted Version

---

**Article:**

Punwong, Paramita, Selby, Katherine Anne [orcid.org/0000-0002-3055-2872](https://orcid.org/0000-0002-3055-2872) and Marchant, Robert [orcid.org/0000-0001-5013-4056](https://orcid.org/0000-0001-5013-4056) (2018) Holocene mangrove dynamics and relative sea-level changes along the Tanzanian coast, East Africa. *Estuarine coastal and shelf science*. pp. 105-117. ISSN 0272-7714

<https://doi.org/10.1016/j.ecss.2018.07.004>

---

**Reuse**

This article is distributed under the terms of the Creative Commons Attribution-NonCommercial-NoDerivs (CC BY-NC-ND) licence. This licence only allows you to download this work and share it with others as long as you credit the authors, but you can't change the article in any way or use it commercially. More information and the full terms of the licence here: <https://creativecommons.org/licenses/>

**Takedown**

If you consider content in White Rose Research Online to be in breach of UK law, please notify us by emailing [eprints@whiterose.ac.uk](mailto:eprints@whiterose.ac.uk) including the URL of the record and the reason for the withdrawal request.

1  
2  
3  
4 1 Holocene mangrove dynamics and relative sea-level changes along the Tanzanian  
5  
6 2 coast, East Africa  
7

8 3 Paramita Punwong<sup>1,2\*</sup>, Katherine Selby<sup>3</sup>, Rob Marchant<sup>2</sup>  
9  
10 4

11  
12 5 <sup>1</sup> Faculty of Environment and Resource Studies, Mahidol University, Nakhon  
13  
14 6 Pathom, 73170, Thailand

15  
16 7 <sup>2</sup> York Institute of Tropical Ecosystems, Environment Department, University of  
17  
18 8 York, York YO10 5NG, UK

19  
20 9 <sup>3</sup> Environment Department, University of York, York YO10 5NG, UK  
21  
22  
23 10

24  
25 11 **Abstract** There is continued uncertainty regarding the rate, timing, duration and  
26  
27 12 direction of Holocene sea-level for the Indian Ocean, and indeed the wider  
28  
29 13 tropical realm. We present the first synthesis, and a new chronology, for  
30  
31 14 Holocene relative sea-level (RSL) using a range sediment cores retrieved from  
32  
33 15 mangrove ecosystems in three locations along coastal Tanzania. This study  
34  
35 16 applies the relationship of ratios between the key mangrove taxa of  
36  
37 17 *Sonneratia*:(*Bruguiera*/*Ceriops*) (S/BC) (ranging from 0 – 22.9) and  
38  
39 18 *Sonneratia*:*Rhizophora* (S/R) (ranging from 0 – 2.29), vegetation and altitude to  
40  
41 19 interpret mangrove dynamics and refine the vertical errors associated with relative  
42  
43 20 sea level change. The variations in mangrove taxa ratios in the sediment cores  
44  
45 21 obtained from each site shows mangrove development at different periods during  
46  
47 22 the Holocene from around 7900 cal yr BP. An early to mid-Holocene RSL rise  
48  
49 23 occurred from ~7900 to ~4600 cal yr BP that may have reached a higher level  
50  
51 24 than present. A lower RSL occurred after 4600 cal yr BP, resulting in mangroves  
52  
53 25 retreating seaward at all three study locations, before a low magnitude RSL rise  
54  
55  
56  
57  
58  
59  
60

26 occurred between 4400 and 2000 cal yr BP. Another RSL rise is recorded at ~  
27 500 cal yr BP before falling to a level lower than present at ~100 cal yr BP. There  
28 is evidence of a recent RSL rise recorded from mangrove ratios during the last  
29 century. In addition, the sedimentation rates among sites are relatively different  
30 due to different altitudinal ranges with freshwater input, sediment supply and  
31 progradation having significantly more effect in the Rufiji Delta (2.1-10.9 mm cal  
32 yr<sup>-1</sup>) than at the Zanzibar sites (0.3-6.6 mm cal yr<sup>-1</sup>).

34 Keywords: Indian Ocean, pollen-vegetation relationships, far-field locations,  
35 Zanzibar, Rufiji Delta

37 \*Corresponding author.

38 E-mail: [punnbio@gmail.com](mailto:punnbio@gmail.com); [paramita@mahidol.edu](mailto:paramita@mahidol.edu)

## 1. Introduction

Relative sea-level (RSL) (the height of the ocean with respect to the surface of the solid Earth) has fluctuated over time that has resulted in geophysical and ecological changes (Pirazzoli, 1991). Far-field sites, located at a distance from the major ice sheets, are important locations for reconstructing RSL changes. Far-field locations can provide important constraints on global RSL change when combined with more intensively studied temperate areas, where coastal adjustments following removal of ice loading are most acute, especially during the mid and late Holocene (Milne and Mitrovica, 2008).

Holocene RSL changes in far-field locations result from eustatic changes, equatorial syphoning and hydro-isostasy (continental levering) (Mitrovica and Milne, 2002; Milne and Mitrovica, 2008). Equatorial ocean syphoning results from collapsing forebulges at the near-field continental margins that cause RSL fall to be recorded in far-field locations (Mitrovica and Peltier, 1991). Continental levering occurs when there is water loading due to deglaciation, that causes continental subsidence and an uplift of the adjacent continents, inducing RSL fall at areas distant from the continental margins (Lambeck and Nakada, 1990; Mitrovica and Milne, 2002; Gehrels and Long, 2008). RSL records from far-field locations have been produced from various locations including the Indian Ocean (Katupotha and Fujiwara, 1988; Banjeree, 2000), Southeast Asia (Hanebuth et al., 2000; Horton et al., 2005; Bird et al., 2007) and Australia (Lambeck and Nakada, 1990; Larcombe et al., 1995; Lewis et al., 2013). Holocene RSL changes have been reconstructed from Australia using a range of coastal and coral reef proxies; some studies suggest a highstand at ~6000 cal yr BP (Lambeck and Nakada, 1990; Larcombe et al., 1995), whereas others indicate a later highstand around 3900 cal

64 yr BP (Baker et al., 2001). A review of geo-chronological data from along the  
65 southeast coast of Australia, indicates a highstand from 7700 cal yr BP that lasted  
66 until about 2000 cal yr BP, before falling to the present-day level (Sloss et al.,  
67 2007). In the northern Indian Ocean, two mid-late Holocene highstands, one at  
68 7300 cal yr BP and another at 4300 cal yr BP, have been recorded from beach  
69 ridges and coral terraces along the east coast of India (Banerjee, 2000). These  
70 highstands were also recorded from corals and marine shells along the southwest  
71 and south coasts of Sri Lanka (Katupotha and Fujiwara, 1988) occurring at 6500  
72 cal yr BP and 3200 cal yr BP.

73 Clearly far-field RSL records are of immense value for understanding and  
74 constraining sea level records but there is a range of timings and duration of these.  
75 In this paper we present evidence of RSL changes derived from three mangrove  
76 sediment records (Punwong et al., 2012; 2013a; 2013b) from sites on the  
77 Tanzanian coast. Combined, these data provide the first sea-level curve and a  
78 refined chronology for Holocene RSL and coastal changes for Tanzania. This  
79 study also uses the relationship between ratios of key mangrove taxa, vegetation  
80 and altitude to interpret mangrove dynamics and refine the vertical errors of RSL  
81 change. Holocene RSL changes are integrated with existing RSL reconstructions  
82 from the region to develop a reconstruction of Holocene RSL changes across the  
83 Southwest Indian Ocean.

#### 85 1.1. Sea-level history in the southwest Indian Ocean

86 The record of Holocene RSL change along the East African coast, situated  
87 in the tectonically stable (Woodroffe and Horton, 2005) Southwest Indian Ocean,  
88 is poorly constrained (Pirazzoli, 1991; Camoin et al., 2004). Reconstructed RSL

changes are available from only a few locations and use a range of different proxies (Figure 1a). Previous studies of RSL change on the continental coasts of east and southeast Africa (Mozambique and South Africa) indicate that RSL rose rapidly during the early Holocene and reached the present level by the mid Holocene (Jaritz et al., 1977, Ramsay, 1995; Ramsay and Cooper, 2002; Norström et al., 2012). Mid Holocene highstands of up to 3.5 m above the present level were recorded by 5000 cal yr BP, followed by subsequent falls to the present level in the late Holocene. A different RSL reconstruction derived from coral from the offshore islands (Mauritius, Mayotte and Réunion Island) shows that a rapid RSL rise occurred during the early Holocene reaching present level at ~3000 cal yr BP with no evidence for a mid Holocene highstand (Camoin et al., 1997; 2004; Colonna et al., 1997; Zinke et al., 2003). Although all RSL studies within this region record an early Holocene RSL rise, there is considerable uncertainty on the amplitude and timing of this. The varied environmental settings and distances from formerly glaciated areas would result in different isostatic contributions to RSL changes. For example, it is thought that small offshore volcanic islands are less affected by hydro-isostatic adjustment than those studies from continental locations due to the effects of continental levering during the mid and late Holocene (Camoin et al., 2004; Lambeck and Nakada, 1990; Mitrovica and Milne, 2002; Milne and Mitrovica, 2008). The different proxies used make it likely that the sea-level index points may not be comparable and some sea-level index points may have large indicative ranges and different degrees of precision (Jaritz et al., 1977; Ramsay, 1995; Ramsay and Cooper, 2002; Woodroffe and Horton, 2005; Norström et al., 2012).

## 1.2. Mangrove as sea-level indicators

Research on RSL reconstruction from far-field locations has traditionally focused on coring and dating corals (Pirazzoli, 1988; Fairbanks, 1989; Colonna et al., 1997; Camoin et al., 1997, 2004). However, sediments that accumulate within mangrove ecosystems can also be used to reconstruct RSL and coastal changes. Mangrove ecosystems are found in coastal tropical regions along the margins of the sea and lagoons; they are characterised by evergreen trees and shrubs that are physiologically and morphologically adapted to grow in the sub-tropical to tropical intertidal zone between mean sea level and the high water of spring tide (Woodroffe and Grindrod, 1991; Blasco et al., 1996; Ellison and Farnsworth, 2001; Ellison, 2008). Mangrove ecosystems respond to changes in sea level by migrating landwards with a rise in sea level or seawards with a fall (Gilman et al., 2008). Mangrove community composition is able to keep pace with sea-level changes (McIvor et al., 2013). For mangroves to be able to withstand sea level rise, the rates of sedimentary accretion within the mangrove has to be equivalent to the rate of sea-level rise (Ellison, 2015), otherwise mangroves may undergo *in situ* drowning leading to weakened root structures, dieback and disappearance (Gilman et al., 2008).

Santisuk (1983) and Watson (1928) classified mangroves into a series of inundation class zones according to ecological preference to monthly inundation frequency. *Rhizophora mucronata*, *Avicennia marina*, *Sonneratia alba*, *Bruguiera gymnorhiza* and *Ceriops tegal* are classified as true mangroves or mangroves. The term true mangroves are also defined as mangroves representing trees and shrubs growing in the areas inundated by the normal to all high tides. Back mangroves such as *Heritiera littoralis* and *Acrostichum aureum* are plants

growing in the areas inundated by the sea only during spring high tides, exceptional high tides, or during cyclones. The dominance of mangrove species which occurs in zones throughout the mangrove ecosystem can thus be an indicator of sea-level fluctuations by comparing the relationships between contemporary vegetation assemblages and their inundation frequency with respect to sea level.

Mangrove pollen has previously been used to reconstruct compositional changes in mangrove ecosystems (e.g. Cohen et al., 2005; Horton et al., 2005; Vedel et al., 2006; Tossou et al., 2008; Hait and Behling, 2009) including in East Africa (Punwong et al., 2012; 2013a; 2013b). Engelhart et al. (2007) developed a transfer function from a modern analogue of mangrove surface pollen assemblages that has been used to predict the palaeo mangrove elevation with precision of  $\pm 0.22$  m. A contemporary study into the relationships between mangrove pollen in surface sediment samples and the composition of the vegetation indicated that majority of pollen was local in origin reflecting vegetation in close proximity to the sampling sites (Punwong et al., 2013a, 2013b). Pollen accumulated in sediments underlying mangroves, in combination with an understanding of the present relationship of mangrove composition to the altitude of present sea level, can be used to reconstruct RSL fluctuations (Ellison, 1989; 2005; 2008; Punwong et al., 2012; 2013a; 2013b).



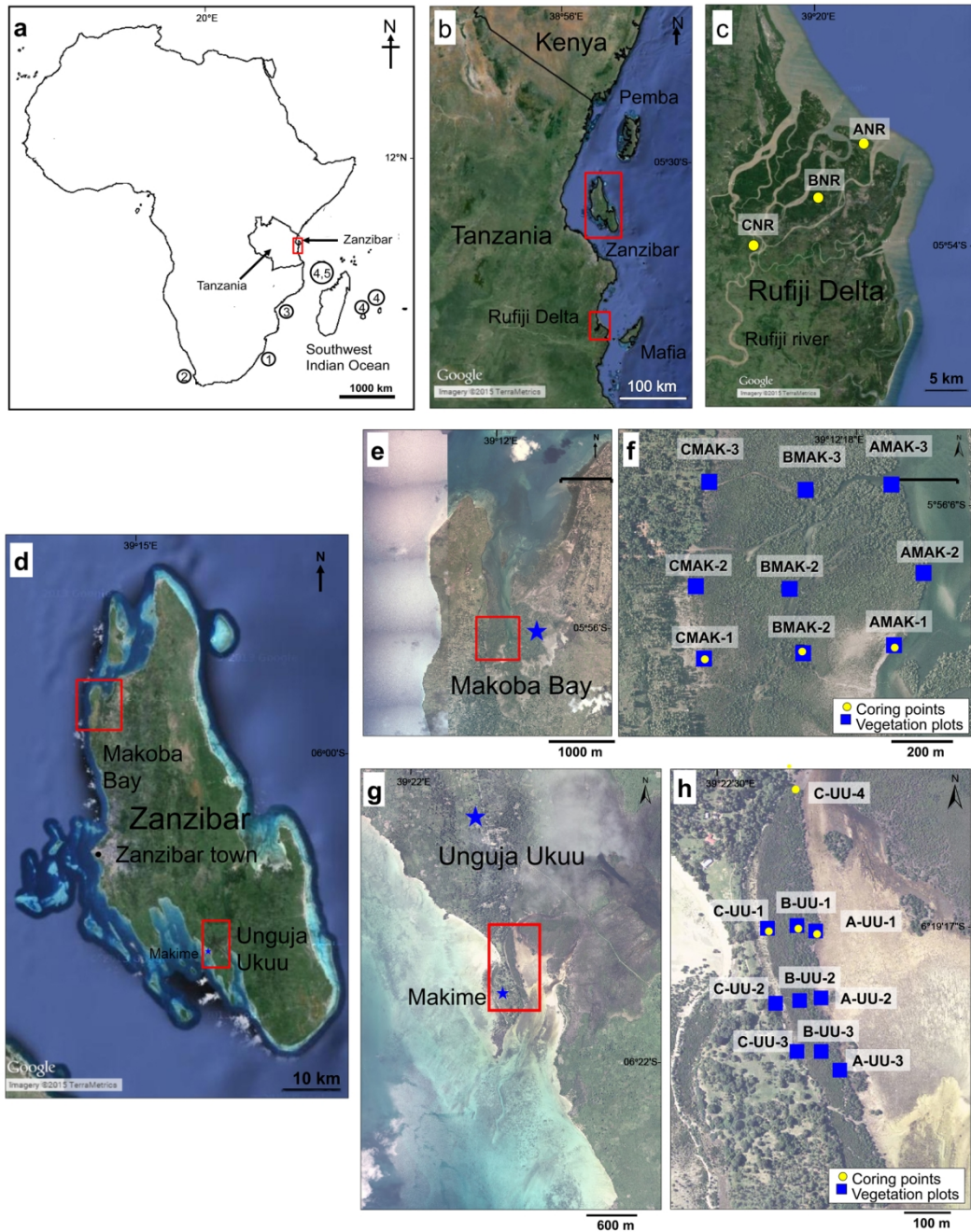


Figure 1. (a) Map of the Southwest Indian Ocean showing the location of Tanzania and previous sea level studies: (1) Ramsay and Cooper (2002), (2) Compton (2001), (3) Jaritz et al. (1977), (4) Colonna et al. (1996); Camoin et al. (1997), (5) Zinke (2000); Zinke et al. (2003). (b) Map of the coast of Tanzania showing the location of the Rufiji Delta (c) and Zanzibar (d). Inset e, f, g and h show where the sedimentary cores were taken and the location of vegetation plots located in Makoba Bay and Unguja Ukuu respectively.

167

## 168 2. Study sites

169

### 170 2.1. Geology and geomorphology

171 The three sites investigated are all characterised by mangrove forest and  
172 located in the northern Rufiji Delta (Tanzanian mainland), Makoba Bay and  
173 Unguja Ukuu (Unguja island, Zanzibar) (Figure 1b-h). The Rufiji Delta consists  
174 of mangrove forest that grades into paddy fields at higher elevations and supports  
175 the largest expanse of estuarine mangrove along the East African coast  
176 (Nshubemuki, 1993; Fisher et al., 1994; Richmond et al., 2002; Masalu, 2003;  
177 Mangora et al., 2016). The deltaic area is covered by fluvial sand, silt and clay  
178 (Semesi, 1992) (Figure 1c). A series of sand spit islands and submerged sand bars  
179 have formed parallel to the seaward margins (Fisher et al., 1994), while clayey  
180 silts and silty clays containing organic matter characterise the mangrove  
181 sediments. The average tidal range is 2 - 2.5 m and approximately 3.3 - 4.3 m on  
182 high spring tides (Francis, 1992; Fisher et al., 1994; Richmond et al., 2002).

183 Unguja Island (Zanzibar) is located on the continental shelf some 40 km  
184 from the mainland. The island has been periodically part of the mainland when  
185 sea level was 30-40 m below present sea level and the last separation from the  
186 mainland by sea-level inundation of the Zanzibar channel occurred at the end of  
187 the Pleistocene to early Holocene (Prendergast et al., 2016). Most of Unguja  
188 consists of Pleistocene reef limestone often outcropping on the east coast  
189 (Shunula, 2002) with alluvial deposits locally present (Schlüter, 1997; Arthurton  
190 et al., 1999) although there are no large rivers (Shunula, 2002). It is influenced by  
191 a semi-diurnal tide, ranging from 2 m on neap tide to 4 m on spring tide

(Mwandya et al., 2010). The study areas are located in the northwest of Makoba Bay (Figure 1d; 1e) and the east Makime headland of Unguja Ukuu (Figure 1d; 1g).

## 2.2. Climate

The rainfall pattern within the Rufiji Delta and on Zanzibar is largely controlled by the north and south migration of the Inter-tropical Convergence Zone (ITCZ). For the Rufiji delta, the northeast monsoon prevails from December to April bringing heavy rainfall (Goudie, 1996; Nicholson, 2001) and the southeast monsoon dominates from May to November bringing less rainfall (Fisher et al., 1994; Richmond et al., 2002). The average annual rainfall is about 1200 mm yr<sup>-1</sup> (Semesi, 1992) and the temperature range throughout the year is 24 - 31 °C (Richmond et al., 2002). For Zanzibar, the northeast and southeast monsoons bring the long rains from March to May and short rains from October to December (Machiwa and Hallberg, 1995; Mwandya et al., 2010). The mean annual rainfall is about 1500 -1800 mm yr<sup>-1</sup> (Knopp et al., 2008) and the average temperature range throughout the year is about 27 - 30 °C (Machiwa and Hallberg, 1995).

## 3. Methodology

### 3.1. Coring

Three sediment cores were retrieved from each site at a seaward, central and landward location using a Russian corer along a transect perpendicular to the coastline through the centre of mangrove forests to reduce the influence of local

land-based edge effects such as erosion or progradation from creeks (Ellison, 2008). The core depths varied between 1 to 4.5 m (Table 1) and each site was cored until the sediment became impenetrable or bedrock was reached (Punwong et al., 2012; 2013a; 2013b). The transect length varied depending on the nature of the environmental setting and the extent of the mangrove area; this extended along 20 km in the northern Rufiji Delta (ANR, BNR, CNR), 600 m in Makoba Bay (AMAK-1, BMAK-1, CMAK-1) and 80 m at Unguja Ukuu (A-UU-1, B-UU-1, C-UU-1) (Figures 1c; 1f, 1h, Table 1). An additional sediment core was retrieved from Unguja Ukuu (C-UU-4) at a location away from the transect as it represents a longer sediment record than the other three cores.

### 3.2. Vegetation plots

To study the relationship between mangrove species composition, pollen accumulating in the sediment and RSL, nine 20 m<sup>2</sup> vegetation plots were set up to establish species percentages along an altitudinal gradient. At the three sites, there was considerable variation in the horizontal distance covered to accommodate the full range of the upper and the lower limits of mangroves. In the Rufiji Delta, the vegetation survey transect along the large riverine mangrove system with freshwater inputs covered 20 km. As the consequence, we were not able to carry out adequate vegetation surveys and to set up plots within the restricted fieldwork time frame. On Zanzibar the transects extended between 80 to 600 m of fringing mangroves characterised by a similar composition across the three sites. Given variations in the horizontal distance and vertical range, the mangrove gradient in Zanzibar is considered to be steeper than the Rufiji Delta. A more detailed study at both sites in Zanzibar allowed the ecosystem and structural composition at different levels of sea-level inundation to be determined and inform the

reconstruction of past RSL fluctuations. Vegetation in nine 20 m<sup>2</sup> nested quadrats was surveyed and recorded and surface sediment samples were collected (Figures 1f, 1h) from three seaward, three central and three landward sites, then considered to be an upper intertidal, a middle intertidal and a lower intertidal mangrove classes, respectively. Five cm<sup>3</sup> of surface samples from the four corners and centre of each plot were collected and subsequently used to study the relationship between pollen presence and vegetation coverage. Altitudinal heights were obtained using a differential GPS (dGPS model Leica TCRA total station and Leica System 500 base and receiver with a manufacturer quoted vertical precision of  $\pm 0.001$  m). Initial calibration of the dGPS occurred against recognised National Datum benchmarks and subsequently all coring sites, vegetation plots and full range of mangrove sites were levelled and calibrated to mean tide level (MTL) (based on Admiralty Tide Tables, 2014). These altitudes were determined relative to a benchmark at Kibiti for the Rufiji Delta using a known actual base station Triangulation point (TTP 353) and the Ministry of Lands and the Environment Benchmark (Zanzibar).

### 3.3. Palaeoecological analysis

The cores were sub-sampled every 10 cm and the volume of each subsample was approximately 2 cm<sup>3</sup> for pollen analysis (Punwong et al., 2012; 2013a; 2013b). The relationship between pollen assemblages and vegetation composition was determined using three pollen association indices that reflect how accurately pollen types reflect the abundance of their parent plant (Davis, 1984). The three indices are ‘association index’ representing similar presence of the pollen and the associated plant in the vegetation, ‘under-representation index’ representing

pollen percentages that are much lower than plant percentages, and ‘over-representation index’ representing pollen percentages that exceed plant percentages (Davis, 1984). Pearson’s Correlation Coefficients were used to describe the relationship between pollen percentages extracted from the surface sediment and plant percentages from the nine vegetation plots in Makoba Bay and Unguja Ukuu.

### 3.4. Chronology

Twenty-six bulk sediment samples were selected for AMS dating and submitted to the Radiocarbon Dating Laboratories at the University of Waikato, New Zealand and the CHRONO Centre, Queen’s University Belfast, UK. At the start of the laboratory work, dates were obtained from the base of the core with targeted dating from different stratigraphic boundaries and key biostratigraphical horizons occurring as the research developed. Additionally, nine dates from AMAK-1 and BMAK-1 cores were obtained on organic concentrate samples following Woodroffe et al. (2015a). Each 1 cm<sup>3</sup> bulk sediment was deflocculated using Na<sub>4</sub>P<sub>2</sub>O<sub>4</sub>/ NaOH, heated with 10% HCl and sieved through a 10, 63 and 90 µm mesh. The 10-63 µm sieving fraction was selected for dating as it contained fine organic material and pollen (Woodroffe et al., 2015a). The organic concentrate samples were submitted for dating to the Natural Environment Research Council (NERC) Radiocarbon Facility (East Kilbride) for AMS dating (NERC Radiocarbon Facility Allocation 1608.0312). All dates were calibrated using the southern hemisphere calibration Shcal04 curve (McCormac et al., 2004) using the software OxCal v4.10 (Bronk-Ramsey, 2009).

## 4. Results

### 4.1. Stratigraphy

Detailed stratigraphic descriptions and diagrams have been previously published (Punwong et al., 2012; 2013; 2013b). There were no abrupt stratigraphic boundaries between the units; they were gradational in all ten cores. The basal unit of BNR and CNR in the northern Rufiji Delta was comprised of organic matter and silt (Punwong et al., 2012). Organic matter amount, including root fragments, increased towards the top of the cores where wood and bark fragments were also present.

In the three cores retrieved from Makoba Bay, the deepest sediment was grey silt with some shell fragments (Punwong et al., 2013b). In cores AMAK-1 and BMAK-1 the silt unit was overlain by a peat unit containing woody root fragments and fine sand. Sand was found in the uppermost unit of all three cores.

The basal unit of A-UU-1, B-UU-1 C-UU-1 sediment cores from Unguja Ukuu was grey sand and silt with silt as the basal unit in C-UU-4 (Punwong et al., 2013a). All basal units were overlain by peat with woody root fragments. Some small shell fragments were also found in this unit in A-UU-1 and B-UU-1. Peat layers with sand and small fragments of woody plant roots alternated with organic sand layers throughout the sediment column in all four cores. Sand containing small fragments of woody plant root formed the top unit of B-UU-1, C-UU-1, and C-UU-4 while silt characterised the top unit of A-UU-1.

### 4.2. Pollen analysis and vegetation survey

Fossil pollen and spores were identified and placed into five main ecological groups: mangroves, back mangroves, terrestrial herbaceous, pteridophytes and unidentifiable pollen; the first two (mangroves, back mangroves), denote a tolerance to sea-water inundation (Punwong et al., 2012; 2013a; 2013b). Terrestrial taxa consisted solely of terrestrial herbaceous plants such as grasses and sedges that are not tolerant of salinity. An understanding of the contemporary mangrove species within the zones is used to underpin the interpretation of ecosystem and environmental changes through the fossil record. Nine mangrove species found in Tanzania within a zonation scheme developed through a combination of Watson's (1928) and Santisuk's (1983) inundation classes (mangroves and back mangroves) and field-based observations of modern ecological occurrences of mangrove taxa (Figure 2a) (Punwong et al., 2012; 2013a; 2013b) are therefore used as a modern analogue of mangrove pollen to interpret sea level. Low mangrove diversities and a linear relationship between contemporary mangrove habitat and inundation frequency negates the need for the use of transfer functions (Ellison, 1989; Engelhart et al., 2007).

Contemporary vegetation assemblages observed in the field based on Watson and Santisuk (1928) classes revealed a distinct vertical relationship with present sea level. The altitude of the upper and lower limits of the mangrove areas was +1.67 m to +3.47 m mean tide level (MTL) in the northern Rufiji Delta, -1.63 m to +1.47 m MTL in Makoba Bay, and -0.03 m to +1.87 m MTL at Unguja Ukuu. The altitudinal variation of the upper and lower limits of the mangrove areas at the three sites is due to different mangrove systems and environmental settings. In the northern Rufiji Delta, an estuarine mangrove ecosystem exists while at Unguja Ukuu and Makoba Bay, fringe mangroves with less freshwater



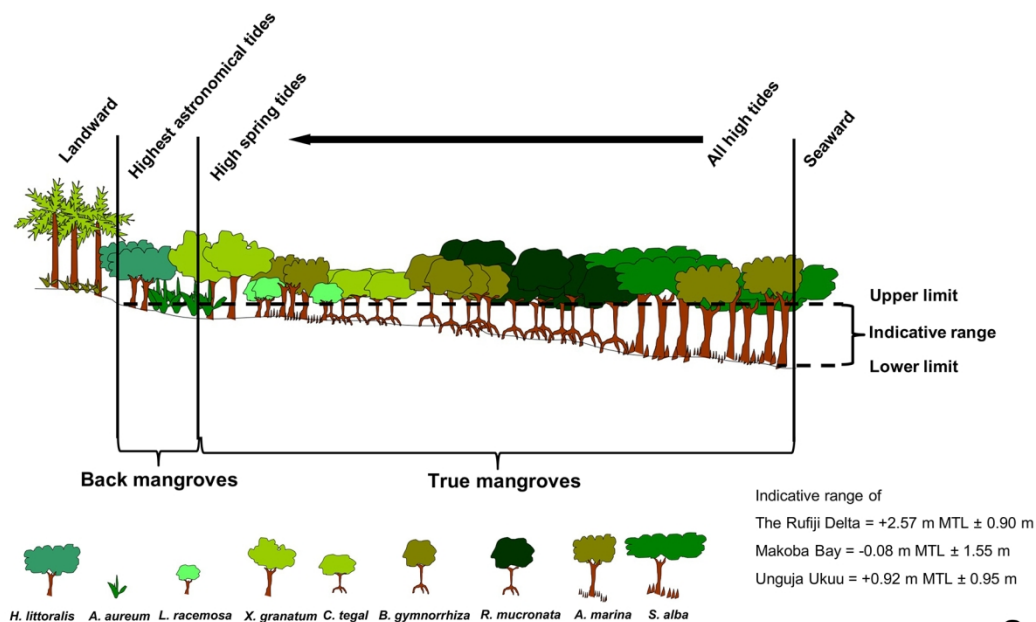
input are found. For Makoba Bay we acknowledge it is unusual for mangroves to grow at -1.63 m MTL and is most likely caused by the geomorphology of the tidal creek system that allows seaward mangrove species, e.g. *Sonneratia alba*, to colonise altitudes below MTL.

The indices of pollen association (Davis, 1984) and correlation between the contemporary mangrove pollen records and contemporary vegetation showed that fossil mangrove pollen in Zanzibar have a close correlation between representivity in pollen spectra and the actual vegetation and can be used to reconstruct coastal ecosystem dynamics (Punwong et al., 2013a; 2013b). Strikingly, there are some notable changes between the percentages of *Sonneratia alba* and *Bruguiera/Ceriops* pollen throughout Zanzibar cores. At the present-day *Sonneratia alba* and *Bruguiera/Ceriops* appear at different altitudes; *Sonneratia alba* occurs in the lower intertidal zone whilst *Bruguiera* and *Ceriops* occur at higher intertidal areas. The relative pollen ratios of *Sonneratia*:(*Bruguiera/Ceriops*) (S/BC ratio) and *Sonneratia*:*Rhizophora* (S/R ratio) of the surface samples from each vegetation plot vary with altitudinal gradient (Table 2). An increase in the ratios of S/BC and S/R indicates a decrease in altitude of the mangrove ecosystem and associated sea level (Table 2). These ratios are applied to infer the mangrove altitude shift within the upper and lower altitudinal limits of the Makoba Bay and Unguja Ukuu study areas as a modern analogue of altitude mangrove classes (Table 2). In Makoba, the S/BC ratios of 5.4 – 22.8 and the S/R ratios of 0.37 – 2.29 represent lower intertidal mangroves; the S/BC ratios of 0.2 – 5.4 and the S/R ratios of 0.04 – 2.29 represent middle intertidal mangroves; the S/BC ratios of 0 – 0.2 and S/R ratios of 0 – 0.04 represent higher intertidal mangroves. At Unguja Ukuu, the S/BC ratios of 0.17 –

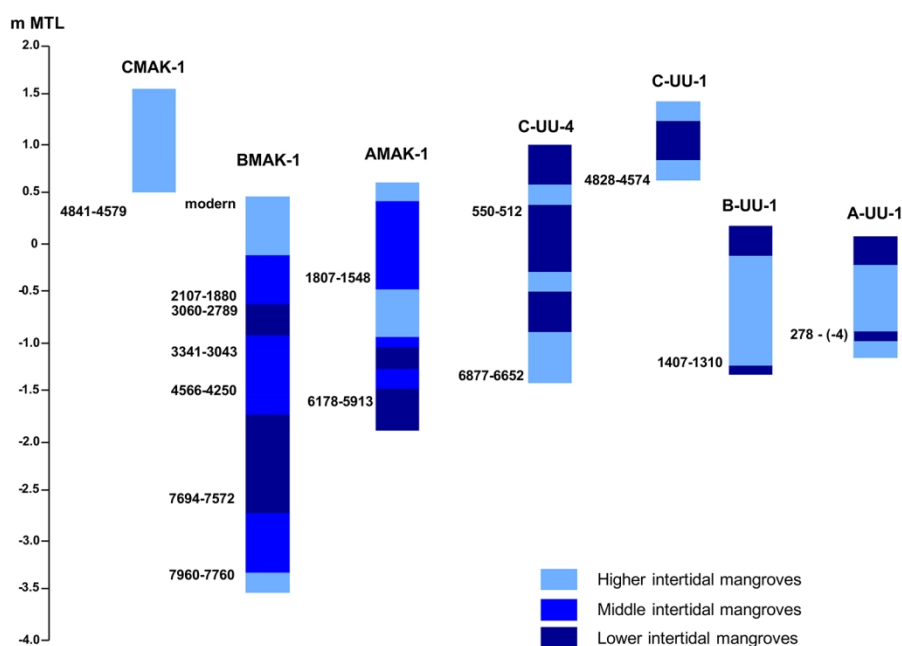
961  
962  
963  
964 366 2.23 and the S/R ratios of 0.20– 0.59 represent lower intertidal mangroves; the  
965  
966 367 S/BC ratios of 0 – 0.17 and the S/R ratios of 0 – 0.20 represent higher intertidal  
967  
968 368 mangroves.  
969

970 369 Therefore, the pollen biostratigraphy as used in this study allows  
971  
972 370 correlation between horizons using the S/BC and S/R ratios of the surface samples  
973  
974 371 within the eighteen vegetation plots that were calculated and used to characterise  
975  
976 372 the mangrove position of the reconstructed past mangrove ecosystems. This  
977  
978  
979 373 information is applied to the dated samples (Figure 2b).  
980

981 374  
982  
983  
984  
985  
986  
987  
988  
989  
990  
991  
992  
993  
994  
995  
996  
997  
998  
999  
1000  
1001  
1002  
1003  
1004  
1005  
1006  
1007  
1008  
1009  
1010  
1011  
1012  
1013  
1014  
1015  
1016  
1017  
1018  
1019  
1020



a



b

375

376 Figure 2. (a) Summary cross section showing typical mangrove zonation and

377 response of this to RSL change in Tanzania developed from Watson's (1928) and

378 Santisuk's (1983) inundation classes and field observations with its indicative

379 range. Figure 2. (b) Biostratigraphy of core sites from Makoba Bay and Unguja

380 Ukuu showing paleoenvironmental interpretation in terms of mangrove position

as lower, middle, higher inferred from the ratios of S/BC and S/R. All ages are in cal yr BP developed from Punwong et al. (2013a; 2013b).

| Site                  | Core   | Altitude (m MTL) | $^{14}\text{C}$ yr BP    | (2 $\sigma$ ) Calibrated age range yr BP | Indicative meaning (m MTL) derived from full range of mangrove | RSL (m MTL) derived from full range of mangroves | Mangrove classes with altitudinal range (interpolated from Fig. 2b) | Indicative meaning (m MTL) derived from pollen ratios | RSL (m MTL) derived from pollen ratios | Decompaction correction | Sea-level tendency |
|-----------------------|--------|------------------|--------------------------|--|--|--|---|---|--|-------------------------|--------------------|
| Northern Rufiji Delta | ANR    | 1.61             | 392 $\pm$ 30             | 493-324                                  |  |  |   |   |  |                         |                    |
|                       | BNR    | 3.22             | > 1950 A.D.              |  |  |  |   |   |  |                         |                    |
|                       |        | 2.95             | Failure to make graphite |  |  |  |   |   |  |                         |                    |
|                       |        | 2.34             | 4167 $\pm$ 30            | 4821-4453                                | 2.57 $\pm$ 0.9   | -0.23 $\pm$ 0.9                                  | n/a   | n/a   | n/a                                    | 1.03                    | rise               |
|                       |        | 0.61             | 4751 $\pm$ 30            | 5579-5318                                | 2.57 $\pm$ 0.9   | -1.96 $\pm$ 0.9                                  | n/a   | n/a   | n/a                                    | 0.51                    | rise               |
|                       |        | -0.96            | 4931 $\pm$ 30            | 5711-5486                                | 2.57 $\pm$ 0.9   | -3.59 $\pm$ 0.9                                  | n/a   | n/a   | n/a                                    | 0.02                    | rise               |
|                       | CNR    | 2.33             | > 1950 A.D.              |  |  |  |   |   |  |                         |                    |
|                       |        | 1.06             | 884 $\pm$ 31             | 799-680                                  | 2.57 $\pm$ 0.9   | -1.51 $\pm$ 0.9                                  | n/a   | n/a   | n/a                                    | 0.62                    | fall               |
| Makoba Bay            | AMAK-1 | -0.37*           | 1803 $\pm$ 36            | 1807-1548                                | -0.08 $\pm$ 1.55   | -0.29 $\pm$ 1.55                                 | Middle intertidal (-1.14)-0.57                                      | -0.08 $\pm$ 0.86                                      | -0.29 $\pm$ 0.86                       | 0.46                    | rise               |
|                       |        | -0.41            | 1615 $\pm$ 24            | 1525-1385                                |  |  |   |   |  |                         |                    |
|                       |        | -1.55*           | 5290 $\pm$ 38            | 6178-5913                                | -0.08 $\pm$ 1.55   | -1.47 $\pm$ 1.55                                 | Lower intertidal (-1.61) - (-1.14)                                  | -0.08 $\pm$ 0.23                                      | -1.47 $\pm$ 0.23                       | 0.11                    | fall               |
|                       |        | -1.56            | 5078 $\pm$ 26            | 5892-5659                                |  |  |   |   |  |                         |                    |
|                       | BMAK-1 | 0.39*            | Modern                   |  | -0.08 $\pm$ 1.55   | 0.47 $\pm$ 1.55                                  | Higher intertidal 0.57-1.51   | -0.08 $\pm$ 0.47                                      | 0.47 $\pm$ 0.47                        | 1.19                    | fall               |
|                       |        | -0.54            | 3111 $\pm$ 24            | 3362-3167                                |  |  |   |   |  |                         |                    |
|                       |        | -0.55*           | 2072 $\pm$ 35            | 2107-1880                                | -0.08 $\pm$ 1.55   | -0.47 $\pm$ 1.55                                 | Middle intertidal (-1.14)-0.57                                      | -0.08 $\pm$ 0.86                                      | -0.47 $\pm$ 0.86                       | 0.91                    | fall               |
|                       |        | -0.64            | 1543 $\pm$ 25            | 1477-1305                                |  |  |   |   |  |                         |                    |
|                       | BMAK-1 | -1.16            | 1695 $\pm$ 50            | 1692-1408                                |  |  |   |   |  |                         |                    |
|                       |        | -1.17*           | 3053 $\pm$ 37            | 3341-3043                                | -0.08 $\pm$ 1.55   | -1.09 $\pm$ 1.55                                 | Middle intertidal (-1.14)-0.57                                      | -0.08 $\pm$ 0.86                                      | -1.09 $\pm$ 0.86                       | 0.73                    | rise               |
|                       |        | -1.53            | 309 $\pm$ 23             | 443-289                                  |  |  |   |   |  |                         |                    |
|                       |        | -1.54*           | 4024 $\pm$ 40            | 4566-4250                                | -0.08 $\pm$ 1.55   | -1.46 $\pm$ 1.55                                 | Middle intertidal (-1.14)-0.57                                      | -0.08 $\pm$ 0.86                                      | -1.46 $\pm$ 0.86                       | 0.61                    | rise               |
|                       | CMAK-1 | -2.78            | 6878 $\pm$ 36            | 7735-7582                                |  |  |   |   |  |                         |                    |
|                       |        | -2.79*           | 6847 $\pm$ 39            | 7694-7572                                | -0.08 $\pm$ 1.55   | -2.7 $\pm$ 1.55                                  | Low intertidal (-1.61) - (-1.14)                                    | -0.08 $\pm$ 0.23                                      | -2.70 $\pm$ 0.23                       | 0.24                    | rise               |
|                       |        | -3.52*           | 7092 $\pm$ 38            | 7960-7760                                | -0.08 $\pm$ 1.55   | -3.46 $\pm$ 1.55                                 | Middle intertidal (-1.14)-0.57                                      | -0.08 $\pm$ 0.86                                      | -3.46 $\pm$ 0.86                       | 0.01                    | rise               |
|                       |        | -3.54            | 7202 $\pm$ 30            | 8025-7872                                |  |  |   |   |  |                         |                    |
|                       |        | 0.41             | 5200 $\pm$ 35            | 5991-5751                                |  |  |   |   |  |                         |                    |
|                       |        | 0.18             | 4239 $\pm$ 37            | 4841-4579                                |  |  |   |   |  |                         |                    |
|                       |        | -0.24            | 3117 $\pm$ 35            | 3376-3162                                |  |  |   |   |  |                         |                    |
|                       |        |                  |                          |  |  |  |   |   |  |                         |                    |
| Unguja Ukuu           | A-UU-1 | -0.84            | 169 $\pm$ 22             | 278(-4)                                  | 0.92 $\pm$ 0.95  | -1.76 $\pm$ 0.95                                 | Lower intertidal 0.01-0.21  | 0.92 $\pm$ 0.10                                       | -1.76 $\pm$ 0.10                       | 0.17                    | fall               |
|                       | B-UU-1 | -1.24            | 1534 $\pm$ 23            | 1407-1310                                | 0.92 $\pm$ 0.95  | -2.16 $\pm$ 0.95                                 | Higher intertidal 0.21-1.91   | 0.92 $\pm$ 0.85                                       | -2.16 $\pm$ 0.85                       | 0.04                    | fall               |
|                       | C-UU-1 | 0.57             | 4211 $\pm$ 25            | 4828-4574                                | 0.92 $\pm$ 0.95  | -0.35 $\pm$ 0.95                                 | Lower intertidal 0.01-0.21  | 0.92 $\pm$ 0.10                                       | -0.35 $\pm$ 0.10                       | 0.09                    | rise               |
|                       | C-UU-4 | 0.59             | >1950 AD                 |  |  |  |   |   |  |                         |                    |
|                       |        | 0.39             | 560 $\pm$ 19             | 550-512                                  | 0.92 $\pm$ 0.95  | -0.53 $\pm$ 0.95                                 | Lower intertidal 0.01-0.21  | 0.92 $\pm$ 0.10                                       | -0.53 $\pm$ 0.10                       | 0.47                    | fall               |
|                       |        | -1.29            | 5973 $\pm$ 36            | 6877-6652                                | 0.92 $\pm$ 0.95  | -2.21 $\pm$ 0.95                                 | Higher intertidal 0.21-1.91   | 0.92 $\pm$ 0.85                                       | -2.21 $\pm$ 0.85                       | 0.02                    | rise               |

Table 1. List of radiocarbon dates derived from bulk samples and organic concentrates (marked with asterisks) from three sites. The calibrated ages are shown using the Shcal04 curve (McCormac et al., 2004) within the software

OxCal v4.10 Bronk-Ramsey (2009). RSL dates are also depicted using the indicative range derived from the upper and lower limits of modern mangrove vegetation and altitudinal error derived from the full range of mangroves for the Rufiji Delta and from the pollen ratios for Makoba and Unguja Ukuu.

| Site        | Plot   | Altitude of plot MTL (m) | Altitudinal range of mangrove classes | S/BC ratio | Range of S/BC ratios | S/R ratio | Range of S/R ratios | Mangrove classes  |
|-------------|--------|--------------------------|---------------------------------------|------------|----------------------|-----------|---------------------|-------------------|
| Makoba Bay  | AMAK-3 | -1.61                    | (-1.61) - (-1.14)                     | 22.8       | 5.4-22.8             | 2.29      | 0.37-2.29           | Lower intertidal  |
|             | AMAK-2 | -1.14                    |                                       | 5.4        |                      | 0.37      |                     |                   |
|             | BMAK-3 | -0.55                    | (-1.14) - 0.57                        | 1.3        | 0.2-5.4              | 0.07      | 0.04-2.29           | Middle intertidal |
|             | BMAK-2 | -0.05                    |                                       | 0.2        |                      | 0.04      |                     |                   |
|             | BMAK-1 | 0.42                     |                                       | 0.2        |                      | 0.05      |                     |                   |
|             | AMAK-1 | 0.57                     |                                       | 0.2        |                      | 0.09      |                     |                   |
|             | CMAK-3 | 1.01                     | 0.57-1.51                             | 0          | 0-0.2                | 0         | 0-0.04              | Higher intertidal |
|             | CMAK-1 | 1.48                     |                                       | 0          |                      | 0         |                     |                   |
|             | CMAK-2 | 1.51                     |                                       | 0          |                      | 0         |                     |                   |
| Unguja Ukuu | A-UU-3 | 0.01                     | 0.01-0.21                             | 2.23       | 0.17-2.23            | 0.59      | 0.20-0.59           | Lower intertidal  |
|             | A-UU-1 | 0.07                     |                                       | 0.88       |                      | 0.20      |                     |                   |
|             | B-UU-1 | 0.14                     |                                       | 0.72       |                      | 0.25      |                     |                   |
|             | A-UU-2 | 0.21                     |                                       | 0.17       |                      | 0.33      |                     |                   |
|             | B-UU-2 | 0.86                     | 0.21-1.91                             | 0.04       | 0-0.17               | 0.16      | 0-0.20              | Higher intertidal |
|             | B-UU-3 | 0.99                     |                                       | 0.04       |                      | 0.08      |                     |                   |
|             | C-UU-1 | 1.35                     |                                       | 0.02       |                      | 0.05      |                     |                   |
|             | C-UU-3 | 1.89                     |                                       | 0          |                      | 0         |                     |                   |
|             | C-UU-2 | 1.91                     |                                       | 0          |                      | 0         |                     |                   |

Table 2. Vegetation plots of Makoba Bay and Unguja Ukuu showing *Sonneratia*/(*Bruguiera*/*Ceriops*) (S/BC) and *Sonneratia*/*Rhizophora* (S/R) ratios of surface samples developed from Punwong et al. (2013a; 2013b). The ranges of ratios show the modern altitudinal range and are applied to infer the mangrove position of sediment in core as modern analogue of lower intertidal, middle intertidal, higher intertidal mangrove classes of the area with respect to altitude.

### 4.3. Chronology

Nine radiocarbon dates were obtained from the northern Rufiji Delta (Table 1). The radiocarbon dates indicate sedimentary hiatuses in the upper part of BNR between 46 cm (4821- 4453 cal yr BP) and 19 cm (modern deposition) and between 242 cm (799 - 680 cal yr BP) and 115 cm (modern deposition) in CNR. The dates from 19 cm (BNR) and 115 cm (CNR) are therefore rejected for RSL reconstruction. In ANR there is no pollen record between the depths of 115-150

1201  
1202  
1203  
1204 407 cm. The date from 128 cm of ANR is therefore not applicable for RSL  
1205  
1206 408 reconstruction.

1207  
1208 409 Eleven radiocarbon dates on bulk sediment were obtained from Makoba  
1209  
1210 410 Bay (Table 1). The radiocarbon dates from cores BMAK-1 (96 and 195 cm) and  
1211  
1212 411 CMAK-1 (107 and 172 cm) demonstrate age reversals. Despite their potential,  
1213  
1214 412 mangrove peats are notoriously difficult to date with age reversals common in  
1215  
1216 413 radiocarbon dated sequences, and modern ages often being reported from samples  
1217  
1218 414 collected several decimeters below the ground surface (e.g. Woodroffe and  
1219  
1220 415 Horton, 2005). The likely causes of these dating problems are reworking of  
1221  
1222 416 mangrove sediments through root penetration introducing younger carbon lower  
1223  
1224 417 down in the sediment profile and mixing of older sediments within the upper unit  
1225  
1226 418 (Punwong et al., 2013b; Woodroffe et al., 2015a). The nine dates obtained from  
1227  
1228 419 the organic concentrates reveal a coherent chronology and logical age-depth  
1229  
1230 420 relationship suggesting reliable dates for AMAK-1 and BMAK-1 (Woodroffe et  
1231  
1232 421 al., 2015a). It would therefore appear that the source of contamination, such as the  
1233  
1234 422 penetration of mangrove roots into the sediment matrix and bioturbation at depth,  
1235  
1236 423 taking younger carbon down the core (Punwong et al., 2013b; Woodroffe et al.,  
1237  
1238 424 2015a). We therefore reject the dates on bulk sediments from the cores AMAK-1,  
1239  
1240 425 BMAK-1 and the two reversed dates (at 107 and 172 cm) of CMAK-1 and use the  
1241  
1242 426 organic concentrate dates for RSL reconstruction. In CMAK-1, there is no pollen  
1243  
1244 427 record between the depths of 105-174 cm. The date from 130 cm of CMAK-1 is  
1245  
1246 428 therefore not used for RSL reconstruction.

1247  
1248  
1249  
1250 429 Six radiocarbon dates were obtained from Unguja Ukuu (Table 1). The  
1251  
1252 430 radiocarbon date from core C-UU-4 (42 cm) records modern age deposition,  
1253  
1254  
1255  
1256  
1257  
1258  
1259  
1260

probably due to contamination (as described above) and this date is therefore rejected for RSL reconstruction.

433

#### 434 4.4. RSL and compaction

435 In order to reconstruct RSL changes using mangrove sediments, the upper  
436 and lower limits of mangrove vegetation with reference to the mean tide level  
437 (MTL) is used in order to establish an indicative range for mangroves following  
438 the approach of Woodroffe et al. (2015b) and Hijma et al. (2015). The indicative  
439 ranges for mangrove sediments are  $+2.57 \text{ m MTL} \pm 0.90 \text{ m}$  in the northern Rufiji  
440 Delta,  $-0.08 \text{ m MTL} \pm 1.55 \text{ m}$  in Makoba Bay and  $+0.92 \text{ m MTL} \pm 0.95 \text{ m}$  in  
441 Unguja Ukuu (Table 1; Figure 2a). To reduce the vertical error, where detailed  
442 contemporary vegetation pollen studies were undertaken in Makoba Bay and  
443 Unguja Ukuu, we use the pollen ratios of S/BC and S/R to calculate the altitudinal  
444 ranges of RSL (as described in 4.2 Pollen analysis and vegetation survey). For  
445 example, the radiocarbon date of 1807-1548 cal yr BP occurs at the depth of 0.94  
446 m in AMAK-1 from Makoba Bay; using the pollen ratios of S/BC and S/R  
447 derived from contemporary pollen studies, it is possible that the vegetation at the  
448 depth of 0.94 m represent a middle-intertidal mangrove association (Figure 2b). If  
449 this is related to MTL using the vegetation plot data, the vertical error of the date  
450 becomes  $\pm 0.86 \text{ m}$  derived from the vertical range of the middle-intertidal  
451 mangrove that is  $-1.14 \text{ m MTL}$  and  $+0.57 \text{ m MTL}$  (Table 1 and 2). The indicative  
452 range derived from the upper and lower limit of mangrove vegetation in Makoba  
453 Bay is  $-0.08 \text{ m MTL}$  and therefore the indicative range of RSL from the date is -  
454  $0.08 \text{ m MTL} \pm 0.86 \text{ m}$  (Table 1).

Sediments are susceptible to post-depositional compaction (Bird et al., 2004; Horton and Shennan, 2009). A compaction factor for the mangrove sediment was estimated by comparing the dry bulk density of a compacted sample with the modern sediment sample and found to range from 17-31% (Bird et al., 2004). As this geotechnical technique is beyond the scope of study, the worst-case compaction scenario of Bird et al. (2004) of 31% was adopted for the decompaction correction below the depth dated (Table 1). For example, at the depth 1.07 m of BNR that is 4.50 m in total length, the compaction of mangrove sediment below this depth would be 1.0633 m (31% of 4.50 – 1.07 m) and would be applied to the vertical error in an upward direction. This approach has also been used in mangrove sea-level reconstructions from mangrove deposits in the Seychelles (Woodroffe et al., 2015b).

Vertical errors also include compaction caused by the coring equipment ( $\pm$  0.04 m) (Woodroffe, 2006), levelling errors ( $\pm$  0.051 m), and the vertical range of the radiocarbon date ( $\pm$  0.005 m). Sea-level tendency for each RSL reconstruction is determined (Table 1) by using a combination of stratigraphy and the trend of mangrove pollen-based interpretation from each coring site (Figure 2b).

## 5. Interpretation and discussion

Age-depth plots of the cores indicated that the basal age for each core ranged from ~ 7900 cal yr BP (BMAK-1 of Makoba Bay) to ~100 cal yr BP (A-UU-1 of Unguja Ukuu). A comparison of sedimentation rates showed great variation between the Rufiji Delta and Zanzibar sites (Figure 3). Although the chronology is problematic, it would appear that the sedimentation rate of between 2.1-10.9 mm cal yr<sup>-1</sup> for the Rufiji Delta was considerably higher than that for



1381  
1382  
1383  
1384 480 Makoba Bay and Unguja Ukuu ( $0.3\text{--}6.6\text{ mm cal yr}^{-1}$ ). This enhanced  
1385  
1386 481 sedimentation rate is probably due to the nature of the deltaic mangrove setting  
1387  
1388 482 with river discharge transporting sediment from the wider Rufiji catchment to be  
1389  
1390 483 deposited into the Rufiji Delta (Semesi, 1992; Fisher et al., 1994). The variation in  
1391  
1392 484 sedimentation rates results in different altitudinal ranges of the mangrove areas at  
1393  
1394 485 the three locations with freshwater input, sediment supply and progradation  
1395  
1396 486 having significantly more effect in the Rufiji Delta than at the Zanzibar sites.  
1397  
1398 487 However, given site-specific responses of mangroves relative to sea level, when  
1399  
1400 488 sites are combined, they provide regional RSL reconstruction.  
1401  
1402  
1403 489  
1404  
1405  
1406  
1407  
1408  
1409  
1410  
1411  
1412  
1413  
1414  
1415  
1416  
1417  
1418  
1419  
1420  
1421  
1422  
1423  
1424  
1425  
1426  
1427  
1428  
1429  
1430  
1431  
1432  
1433  
1434  
1435  
1436  
1437  
1438  
1439  
1440

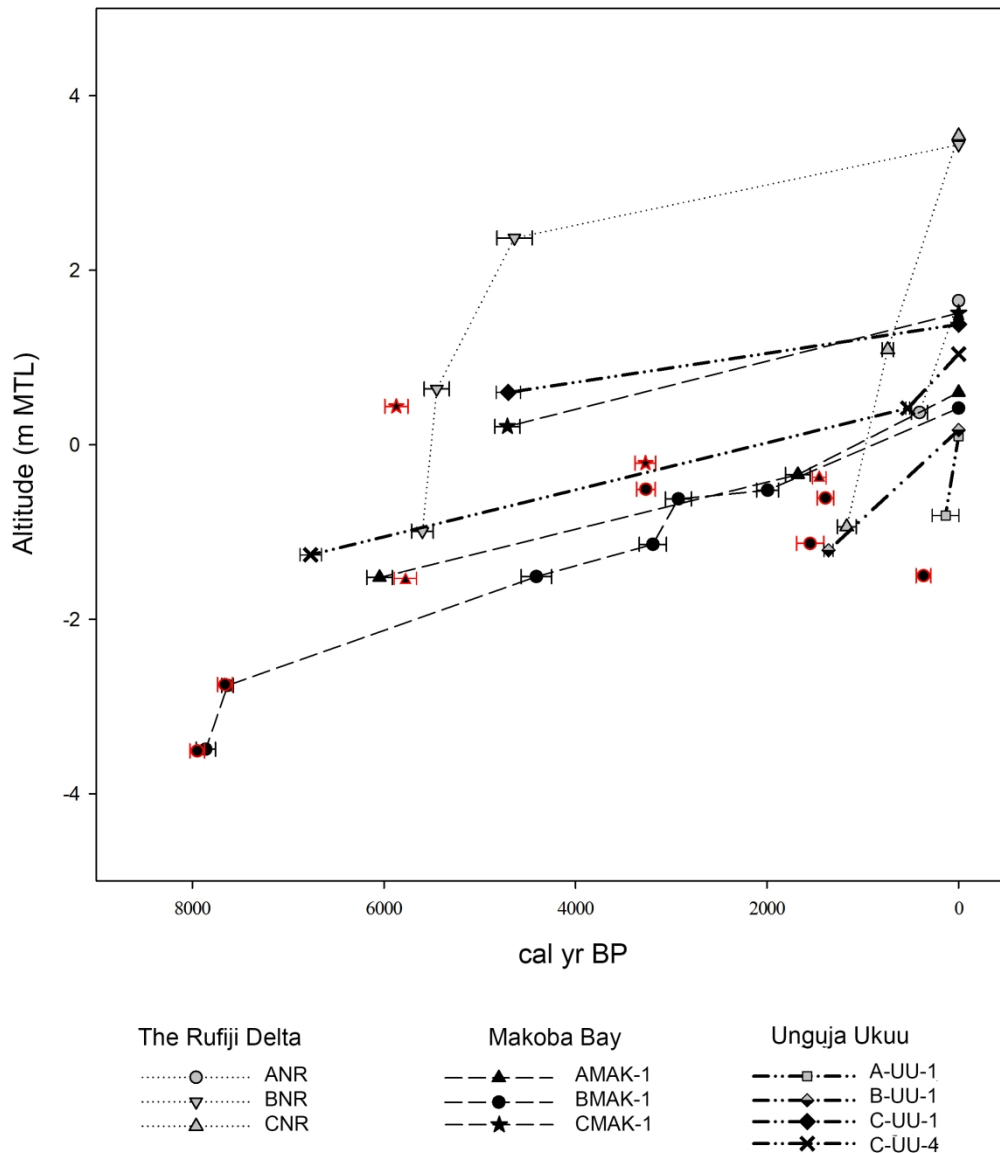


Figure 3. Comparative age-depth plots including rejected dates (in red edge) for the cores analysed in this study. Comparative age-depth (altitude) models for the cores analysed in this study. The top value against the zero origin (cal yr BP) on all such graphs except BMAK-1 does not necessarily represent present day deposition because of potential surface erosion.

### 5.1. Holocene mangrove dynamics

498 Combined palaeoecological records from the three locations provide a new  
499 palaeoenvironmental sea-level synthesis from Tanzania where relatively little is  
500 known about the Holocene mangrove dynamics. The records reveal that mangrove  
501 ecosystems have not remained stable as they responded to wide scale  
502 environmental changes and there are some site-specific responses to  
503 environmental shifts. The results further our understanding of how mangrove  
504 ecosystems reflect environmental variables, and shifts in these, that could help  
505 assess resilience of coastal ecosystems under future climatic scenarios,  
506 particularly sea-level rise (Ellison, 2015).

507 Early to mid Holocene

508 The pollen record of BMAK-1 indicates that mangroves have been present  
509 at Makoba Bay at -3.6 m below MTL since at least ~7900 cal yr BP (Figure 2b).  
510 The ratios of S/BC and S/R suggest that the central core (BMAK-1) location was  
511 colonised by higher intertidal mangroves (Figures 1f, 2b; Table 2) suggesting an  
512 early Holocene RSL rise. A higher RSL rise was then recorded after this period  
513 for a relatively short duration until ~7600 cal yr BP, as mangroves migrated  
514 landward and this area supported middle intertidal mangrove taxa. RSL continued  
515 to rise, as indicated by the ratios of mangrove pollen and the deposition of oyster  
516 shells in BMAK-1b and AMAK-1. This marine transgression caused the  
517 mangrove taxa at these two coring locations to migrate further landwards and  
518 allowed mangroves to establish on the headland of Unguja Ukuu at -1.3 m MTL  
519 as recorded ~6800 cal yr BP in C-UU-4. After this time, higher intertidal  
520 mangroves recorded in C-UU-4 were replaced by lower intertidal mangrove taxa;  
521 thus contributing to a body of evidence indicating that RSL continued to rise  
522 during the mid Holocene (Camoin et al., 1997; 2004; Zinke et al., 2003; Norström

et al., 2012). It should be noted that the pollen records from both sites in Zanzibar reveals a similar age determination of 5600 cal yr BP and a similar pollen record, lending support to the chronological and sea-level interpretation from BNR in the northern Rufiji Delta (Punwong et al., 2012). The predominance of *R. mucronata* pollen suggests that BNR was located in a low intertidal environment, a further indication of a higher sea level relative to the present day. A mid Holocene RSL rise possibly attained a higher altitude after 4700 cal yr BP resulting in higher intertidal mangroves establishment at 0.5 m above MTL in CMAK-1 and higher intertidal mangrove establishment at 0.6 m MTL in C-UU-1. This mid Holocene RSL rise occurred until prior to ~4400 cal yr BP, when RSL started to fall as indicated by the transition from lower intertidal to middle intertidal mangroves in BMAK-1.

Mid Holocene to the present day

After ~4400 cal yr BP mangrove ecosystem character varied between the sites reflecting different RSL changes. A lower RSL is recorded in Makoba Bay from ~4400 cal yr BP, as indicated by the change in mangrove composition from lower to middle intertidal mangroves in BMAK-1 until ~3200 cal yr BP. This period coincides with a regionally arid phase recorded across East Africa commencing around 4500–4100 cal yr BP (Hassan, 1997; Bonnefille and Chalieu, 2000; Thompson et al., 2002; Marchant and Hooghiemstra, 2004; Kiage and Liu, 2006; Rijdsdijk et al., 2011; de Boer et al., 2015). After 3200 cal yr BP, and prior to 2900 cal yr BP, a RSL rise occurred indicative of a change from middle to lower intertidal mangroves. Mangrove composition subsequently changed to middle intertidal mangroves in AMAK-1 and BMAK-1 (Figure 2b) suggesting a

548 lower RSL as mangroves retreated seaward until the late Holocene ~2000-1700  
549 cal yr BP. However, a sea-level rise is recorded at Unguja Ukuu as lower  
550 intertidal mangroves occupied C-UU-1 and C-UU-4 after the mid Holocene until  
551 ~500 cal yr BP. The apparent discrepancy in RSL between these two sites at  
552 Unguja after 4400 to 1700 cal yr BP is probably due to local processes including  
553 mangrove composition response to sediment input and/or erosion at the sites,  
554 resulting in localised RSL changes.

555         The late Holocene RSL fall is recorded at all three sites. In Makoba Bay,  
556 RSL fell until the present day, as suggested by the change of middle intertidal  
557 mangroves to higher intertidal mangroves in AMAK-1 and BMAK-1. At Unguja  
558 Ukuu, lower intertidal mangroves changed to higher intertidal mangroves after  
559 1400 cal yr BP in B-UU-1. RSL probably continued falling in Unguja Ukuu, as  
560 represented by the change from lower intertidal mangroves to higher intertidal  
561 mangroves after ~500 cal yr BP in C-UU-4, and the presence of more intertidal  
562 mangroves after ~100 cal yr BP in A-UU-1. In the Rufiji Delta, a reduction in  
563 mangrove pollen and increase in back-mangrove and terrestrial grasses in the  
564 landward site (CNR) after 1200 cal yr BP resulted in a shift of mangroves  
565 seaward. RSL then fluctuated, as suggested by changes in the proportions of  
566 mangroves, back-mangrove and terrestrial grasses until prior to 700 cal yr BP.  
567 After 700 cal yr BP, RSL started to fall, as recorded by a gradual change from  
568 mangroves characterised by *R. mucronata* to terrestrial vegetation, and a  
569 replacement of mangroves by recent herbaceous taxa. However, changes from  
570 higher intertidal mangroves to lower intertidal mangroves in A-UU-1, B-UU-1  
571 and C-UU4 at Unguja Ukuu, corresponding to an increase in *A. marina* at the top

of ANR, are likely to represent a signal of sea-level rise during the last few hundred years.

## 5.2. Sea-level reconstruction

The pollen evidence from the Rufiji Delta, Makoba Bay and Unguja Ukuu can be used to reconstruct the Holocene RSL from Tanzania using the upper and lower limits of mangrove vegetation and shift in recognisable salinity tolerance zones of the mangrove ecosystem. The RSL derived from the pollen ratios within the vegetation plots can refine vertical errors (Figure 4). Regardless of site-specific characteristics, it should be noted that all three sites provide evidence for a phase of early-mid Holocene RSL rise and late Holocene RSL fluctuation. The composite RSL curve shows that RSL rise occurred from around 7900 cal yr BP. It is possible that RSL rose and was potentially higher than present at ~4700-4600 cal yr BP. However, when the sites are compared (Figure 4), variations in the rate of sea level rise are noted. In the northern Rufiji Delta, the higher sedimentation rates are probably due to the large freshwater and terrestrial inputs to the system.

The general trend of the early to mid Holocene RSL rise (Figure 4) appears to be in agreement with RSL trends from other locations such as the mainland coast and offshore islands in the Southwest Indian Ocean (Colonna et al., 1996; Camoin et al., 1997; 2004; Zinke et al., 2000; Compton, 2001; Ramsay and Cooper, 2002; Zinke et al., 2003).

The proposed higher than present sea level at around 4700-4600 cal yr BP recorded in Tanzania indicates a similar trend to that recorded from South Africa (Compton, 2001; Ramsay and Cooper, 2002) (Figure 4). The mid Holocene RSL rise in Tanzania is also comparable to a marine transgression phase in

1741  
1742  
1743  
1744 597 Mozambique (Norström et al., 2012) where a highstand is recorded ~6600-6300  
1745  
1746 598 cal yr BP. The mid Holocene transgression is well represented from the Southern  
1747  
1748 599 Hemisphere in far-field locations (Isla, 1989) relating to three possible causes  
1749  
1750 600 including meltwater from late glacial ice sheets (Lambeck and Nakada, 1990;  
1751  
1752 601 Fleming et al., 1998) and/or the Holocene melting of ice sheets from Antarctica,  
1753  
1754 602 Greenland and mountain glaciers during the early Holocene until 5000 cal yr BP  
1755  
1756 603 (Milne et al., 2005).

1758  
1759 604 Evidence from Mauritius, Mayotte and Réunion Island (Camoin et al.,  
1760  
1761 605 1997; 2004; Zinke et al., 2003) suggest no mid Holocene highstand occurred at  
1762  
1763 606 these locations. The differences between the records from the islands and  
1764  
1765 607 Tanzania may result from hydro-isostatic influences relating to the differences in  
1766  
1767 608 the geographical locations of the Tanzanian coast and the islands (Clark et al.,  
1768  
1769 609 1978). The Holocene highstand at small offshore islands is likely to be less  
1770  
1771 610 marked than at the continental margins due to the effects of continental levering  
1772  
1773 611 (Lambeck and Nakada, 1990; Mitrovica and Milne, 2002; Milne and Mitrovica,  
1774  
1775 612 2008). However, the highstand recorded from South Africa is likely to be higher  
1776  
1777 613 than the potential maximum transgression at ~4700 cal yr BP and 4600 cal yr BP  
1778  
1779 614 in Tanzania (Compton, 2001; Ramsay and Cooper, 2002). In addition to eustatic  
1780  
1781 615 changes, a combination of various factors such as hydro-isostasy, thermal  
1782  
1783 616 expansion of sea water caused by warmer ocean temperatures in subtropical  
1784  
1785 617 latitudes (Ramsay, 1995, Woodroffe and Horton, 2005), and the steric expansion  
1786  
1787 618 of sea water (Ramsay, 1995; Compton, 2001) may also be considered as factors  
1788  
1789 619 enhancing the highstand altitude in South Africa.

1792  
1793 620 RSL fell from 4600 cal yr BP to 4400 cal yr BP. After 4400 cal yr BP,  
1794  
1795 621 RSL slightly rose until ~2000 cal yr BP. The RSL record at this time from  
1796  
1797  
1798  
1799  
1800

622 Tanzania correlates well with records from South Africa (Ramsay and Cooper,  
623 2002) and also corresponds with a possible marine transgression with a highstand  
624 from Macassa Bay (Mozambique) between 4000 - 1100 cal yr BP (Norström et  
625 al., 2012). The pollen records from Makoba Bay and C-UU-1 and C-UU-4 of  
626 Unguja Ukuu indicate that mangrove development continued after the mid  
627 Holocene RSL rise indicating a sustained higher level that did not fall until the  
628 late Holocene ~2000 cal yr BP. This may have allowed suitable conditions for  
629 mangroves to establish at A-UU-1 and B-UU-1 and may correspond to the  
630 progradation of beach plains that is recorded in Zanzibar (Arthurton, 2003).

631 The late Holocene RSL record after 2000 cal yr BP until 100 cal yr BP  
632 correlates well with the RSL records from South Africa (Compton, 2001; Ramsay  
633 and Cooper, 2002) and Mozambique (Norström et al., 2012) (Figure 4). A lower  
634 sea level occurred in Tanzania until 1400 - 1200 cal yr BP; this RSL fall is also  
635 recorded in northeastern South Africa ~1400 cal yr BP to the present (Ramsay and  
636 Cooper, 2002). We acknowledged that potential sea-level fall would correspond to  
637 climatically cold phases and sea-level rise to warm phases, as a result of the  
638 glacial eustasy (Oerlemans, 2001). Changes in rainfall can also cause local  
639 eustatic sea-level changes (Mörner, 1996). However, easternmost East Africa  
640 experienced drought during the Medieval Warm Period (MWP) (900 - 700 cal yr  
641 BP) and wet conditions during the Little Ice Age (LIA) (700 - 100 cal yr BP)  
642 (Verchuren et al., 2000). These phases are contrast with our records of sea-level  
643 transgression after 1200 - 500 cal yr BP and sea-level regression from 500 - 100  
644 cal yr BP. Archaeological sites in Unguja Ukuu indicate that RSL was  
645 approximately -0.5 m below the present level between ~1300 - 1000 cal yr BP  
646 (Mörner, 1992). This is in good agreement with the reconstruction from the three



1861  
1862  
1863  
1864 647 sites studied suggesting RSL did not attain present sea level between 1400-1200  
1865  
1866 648 cal yr BP (Figure 4).  
1867

1868 649 A further RSL rise occurred after 1200 to ~700 - 500 cal yr BP and it is  
1869  
1870 650 likely that RSL was below the present sea level. This concurs with records from  
1871  
1872 651 ruins in southeastern Tanzania (Kilwa) suggesting RSL was about -1 m below the  
1873  
1874 652 present level between 800- 600 cal yr BP (Mörner, 1992). After this period, RSL  
1875  
1876 653 fell until ~100 cal yr BP when sea level was lower than the present day. This is in  
1877  
1878 654 good agreement with a study of raised terraces along the Kenyan coast indicating  
1879  
1880 655 that RSL started to fall 500 years ago (Åse, 1978; 1981). In contrast, data from  
1881  
1882 656 Mozambique (Norström et al., 2012) and southern Langebaan Lagoon in South  
1883  
1884 657 Africa (Compton, 2001) show somewhat conflicting results from the Tanzanian  
1885  
1886 658 data indicating RSL fell after 1200 cal yr BP. After 100 cal yr BP, RSL rose until  
1887  
1888 659 the present day corresponding to the onset of recent sea-level rise from the 19<sup>th</sup>  
1889  
1890 660 century (Stocker et al., 2013) as recorded in Kenya between 1986-2002 (Kibue,  
1891  
1892 661 2006). However, a recent sea-level fall was observed in Zanzibar between 1985-  
1893  
1894 662 2001 (Permanent Service for Mean Sea Level) before rising trend was observed to  
1895  
1896 663 the present day. In addition, it should be noted that Makoba and Unguja Ukuu  
1897  
1898 664 which all are on the west cost of Unguja Island and separated by 40 km shows  
1899  
1900 665 different RSL especially during the last 2000 years probably due to local  
1901  
1902 666 processes, such as changes in sediment input and/or erosion at the sites.  
1903  
1904  
1905

1906 667 Difficulties encountered in dating suggest additional records and  
1907  
1908 668 chronological control using dating of pollen concentrates is required to determine  
1909  
1910 669 a high-resolution record of mid Holocene sea level and environmental changes.  
1911  
1912 670 Although the evidence from Tanzania demonstrates the site-specific nature of  
1913  
1914 671 responses of mangroves to RSL changes, it does provide a valuable contribution  
1915  
1916  
1917  
1918  
1919  
1920

to patterns of Holocene RSL from “far-field” locations. There is great potential to scale up the type of investigation presented here to other coastal mangrove sites across East Africa, as well as offshore islands. Such an extension to this study would provide an unprecedented regional record of environmental and sea-level changes from a far-field region and allow us to distinguish large and meso-scale regional signals against site-specific responses across East Africa.

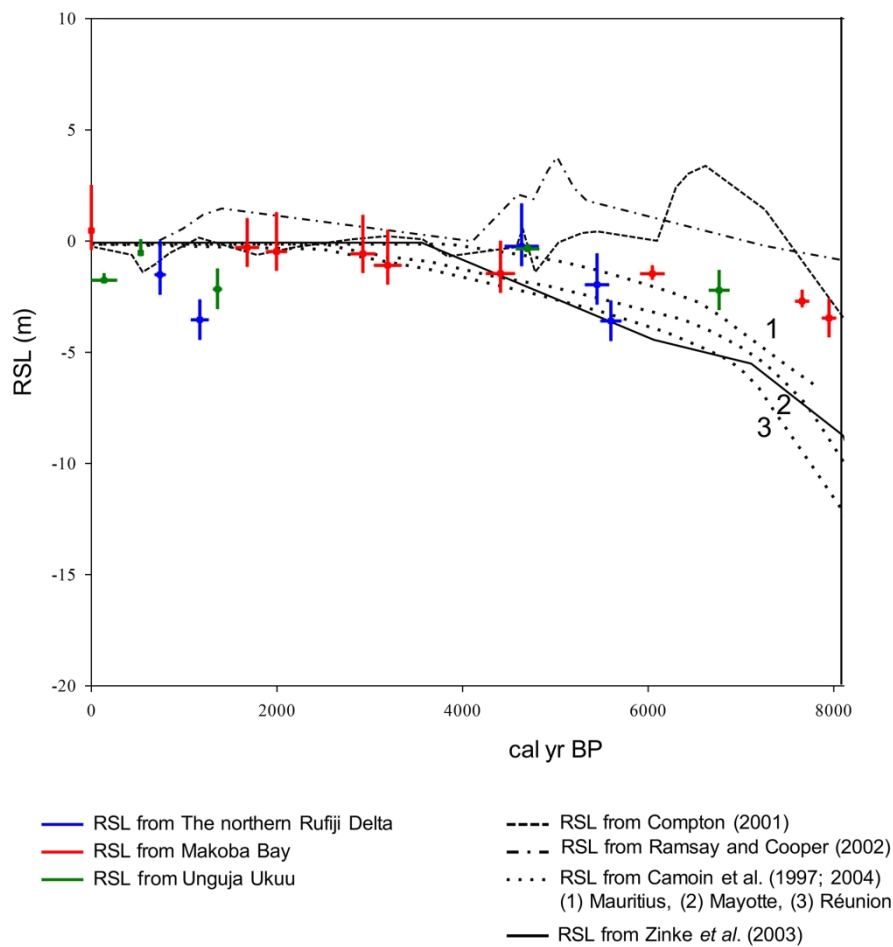


Figure 4. RSL reconstructions from this study along the Tanzanian coast plotted alongside RSL curves from the southwest Indian Ocean region

## 6. Conclusions

1981  
1982  
1983  
1984 683 A reconstruction of Holocene RSL has been derived for coastal Tanzania  
1985  
1986 684 from mangrove ecosystem changes from three sites. The ratios of  
1987  
1988 685 *Sonneratia:(Bruguiera/Ceriops)* and *Sonneratia:Rhizophora* derived from the  
1989  
1990 686 pollen-vegetation-altitude relationships can be used to interpret mangrove  
1991  
1992 687 dynamics and refine the vertical errors of RSL changes derived from mangrove  
1993  
1994 688 sediments. Although the results in part demonstrate the site-specific shifts in the  
1995  
1996 689 upper and lower limits of mangroves relative to sea level, due to responses of  
1997  
1998 690 sediment input and/or erosion at the three sites, they do provide evidence for  
1999  
2000 691 Holocene RSL fluctuations coherent across coastal Tanzania. An early-mid to mid  
2001  
2002 692 Holocene RSL rise occurred from ~ 7900 cal yr BP prior to ~4700-4600 cal yr BP  
2003  
2004 693 when RSL was potentially higher than the present. This period is followed by a  
2005  
2006 694 lower RSL until 4400 cal yr BP when RSL rose until ~2000 cal yr BP.  
2007  
2008 695 Subsequently, late Holocene RSL fluctuations were characterised by RSL rise  
2009  
2010 696 recorded at ~700 - 500 cal yr BP before falling below the present level at ~100 cal  
2011  
2012 697 yr BP. There is evidence of a more recent RSL rise during the last centuries. The  
2013  
2014 698 Tanzanian RSL curve indicates a similar trend to the mid Holocene RSL record  
2015  
2016 699 from South Africa, probably related to similar hydro-isostatic conditions  
2017  
2018 700 representing the apparent Holocene highstand at continental margins due to the  
2019  
2020 701 effects of continental levering. The RSL fall recorded during the last 500 years is  
2021  
2022 702 in good agreement with the records from the Kenyan coast, although data from  
2023  
2024 703 Mozambique and the Langebaan Lagoon in South Africa indicate RSL fell after  
2025  
2026 704 1200 cal yr BP. The difficulties of developing a reliable chronology from  
2027  
2028 705 mangrove environments have previously precluded extensive use of these  
2029  
2030 706 sediment archives for reconstructing RSL changes. Organic concentrate dating  
2031  
2032 707 applied on some of the samples presented here can provide a reliable chronology  
2033  
2034  
2035  
2036  
2037  
2038  
2039  
2040

2041  
2042  
2043  
2044 708 allowing these far-field locations to be fully investigated and used as a proxy for  
2045  
2046 709 reconstructing eustatic sea-level changes. Site-specific signals of RSL change,  
2047  
2048 710 mangrove response to this and the need to further constrain the pollen-vegetation-  
2049  
2050 711 environmental relationships all emphasise the need for further research along the  
2051  
2052 712 East African coast, as well as other “far-field” locations, so that the full potential  
2053  
2054 713 of the mangrove sedimentary sea-level archive can be fully realised.  
2055

2056 714

## 2057 2058 715 Acknowledgements

2059  
2060 716 This work was carried out as a part of doctoral thesis at the University of  
2061  
2062 717 York. Thanks are extended to Mr William Kindeketa and Rebecca Newman for  
2063  
2064 718 their support and assistance throughout the fieldwork. We would like to thank the  
2065  
2066 719 Palynology & Palaeobotany Section, National Museums of Kenya for lending us  
2067  
2068 720 the coring equipment necessary for fieldwork and laboratory work, WWF-  
2069  
2070 721 Tanzania for providing logistical support for the fieldwork in Rufiji Delta and Mr  
2071  
2072 722 Benson Kimeu, Survey/GIS Technician from The British Institute in Eastern  
2073  
2074 723 Africa for conducting the elevation survey. I am grateful to Professor Antony  
2075  
2076 724 Long, Dr. Sarah Woodroffe and Dr. Sanpisa Sritairat for their constructive  
2077  
2078 725 comments on earlier versions of this manuscript. The radiocarbon dates on the  
2079  
2080 726 organic concentrates was funded through NERC Radiocarbon Facility Allocation  
2081  
2082 727 1608.0312. This study was supported by The Royal Thai Government Scholarship  
2083  
2084 728 and the Development and Promotion Science and Technology Talents project.  
2085  
2086 729

## 2087 2088 730 References

2089  
2090 731  
2091  
2092  
2093  
2094  
2095  
2096  
2097  
2098  
2099  
2100

732 Admiralty Tide Tables, 2014. NP203 Admiralty Tide Tables (ATT) Volume 3,  
 733 Indian Ocean and South China Sea (including Tidal Stream Tables).  
 734 Hydrographer to the Navy. Admiralty Hydrography Department. 365 pp.  
 735 Arthurton, R.S., Brampton, A.H., Kaaya, C.Z., Mohamed, S.K., 1999. Late  
 736 Quaternary coastal stratigraphy on a platform-fringed tropical coast- a case study  
 737 from Zanzibar, Tanzania. *Journal of Coastal Research* 15, 635-644.  
 738 Arthurton, R., 2003. The fringing reef coasts of eastern Africa-present processes  
 739 in their long-term context. *Western Indian Ocean Journal Marine Science* 2 (1), 1-  
 740 13.  
 741 Åse, L.E., 1978. Preliminary Report on Studies of Shore Displacement at the  
 742 Southern Coast of Kenya. *Geografiska Annaler, Series A, Physical Geography*,  
 743 60, 3/4, 209-221.  
 744 Åse, L.E., 1981. Studies of Shores and Shore Displacement on the Southern Coast  
 745 of Kenya. Especially in the Kilifi District. *Geografiska Annaler, Series A*,  
 746 *Physical Geography*, 63, 3/4, 303-310.  
 747 Baker, R.G., Haworth, R., Flood, P., 2001. Inter-tidal fixed indicators of former  
 748 Holocene sea levels in Australia: a summary of sites and a review of methods and  
 749 models. *Quaternary International* 83–85, 257–273.  
 750 Banerjee, P.K., 2000. Holocene and Late Pleistocene relative sea level  
 751 fluctuations along the east coast of India. *Marine Geology* 167, 243–260.  
 752 Bird, M. I., L. K. Fifield, S. Chua, Goh, B., 2004. Calculating sediment  
 753 compaction for radiocarbon dating of intertidal sediments. *Radiocarbon* 46(1),  
 754 421–435.

- 2161  
2162  
2163  
2164 755 Bird, M.I., Fifield, L.K., Teh, T.S., Chang, C.H., Shirlaw, N., Lambeck, K., 2007.  
2165  
2166 756 An inflection in the rate of early-mid Holocene eustatic sea-level rise: A new sea-  
2167  
2168 757 level curve from Singapore. *Estuarine, Coastal and Shelf Science* 71, 523–536.  
2169  
2170 758 Blasco, F., Saenger, P., Janodet, E. 1996. Mangroves as indicators of coastal  
2171  
2172 759 change. *Catena* 27, 167–178.  
2173  
2174 760 Bonnefille, R., Chalieu, F., 2000. Pollen-inferred precipitation time-series from  
2175  
2176 761 equatorial mountains, Africa, the last 40 kyr BP. *Global Planet Change* 26, 25–50.  
2177  
2178 762 Bronk-Ramsey, C., 2009. OxCal Program v4.10. Oxford Radiocarbon Accelerator  
2179  
2180 763 Unit, Oxford.  
2181  
2182 764 Camoin, G.F., Colonna, M., Montaggioni, L.F., Casanova, J., Faure, G.,  
2183  
2184 765 Thomassin, B.A., 1997. Holocene sea level changes and reef development in the  
2185  
2186 766 southwestern Indian Ocean. *Coral Reefs* 16 (4), 247–259.  
2187  
2188 767 Camoin, G.F., Montaggioni, L.F., Braithwaite, C.J.R., 2004. Late glacial to post  
2189  
2190 768 glacial sea levels in the Western Indian Ocean. *Marine Geology* 206, 119–146.  
2191  
2192 769 Clark, J.A., Farrell, W.E., Peltier, W.R., 1978. Global changes in post glacial sea  
2193  
2194 770 level: a numerical calculation. *Quaternary Research* 9, 265–287.  
2195  
2196 771 Cohen, M.C.L., Behling, H., Lara, R.J., 2005. Amazonian mangrove dynamics  
2197  
2198 772 during the last millennium: The relative sea-level and the Little Ice Age. *Review*  
2199  
2200 773 *of Palaeobotany and Palynology* 136, 93–108.  
2201  
2202 774 Colonna, M., Casanova, J., Dullo, W.C., Camoin, G., 1997. Sea-level changes and  
2203  
2204 775  $\delta^{18}\text{O}$  record for the past 34,000 yr from Mayotte Reef, Indian Ocean.  
2205  
2206 776 *Oceanographic Literature Review* 44(7), 693–693.  
2207  
2208 777 Compton, J.S., 2001. Holocene sea-level fluctuations inferred from the evolution  
2209  
2210 778 of depositional environments of the southern Langebaan Lagoon salt marsh, South  
2211  
2212 779 Africa. *The Holocene* 11(4), 395–405.  
2213  
2214  
2215  
2216  
2217  
2218  
2219  
2220

780 Davis, O.K., 1984. Pollen frequencies reflect vegetation patterns in a Great Basin  
 781 (U.S.A.) mountain range. *Review of Palaeobotany and Palynology* 40, 295–315.  
 782 de Boer, E.J., Véléz, M.I., Rijdsdijk, K.F., de Louw, P.G., Vernimmen, T.J., Visser,  
 783 P.M., Tjallingii, R. and Hooghiemstra, H., 2015. A deadly cocktail: How a  
 784 drought around 4200 cal. yr BP caused mass mortality events at the infamous  
 785 ‘dodo swamp’ in Mauritius. *The Holocene*, 25(5), 758–771.  
 786 Ellison, A.M., Farnsworth, E.J., 2001. Mangrove communities. In: Bertness,  
 787 M.D., Gaines, S.D., Hay, M.E. (Eds.). *Marine Community Ecology*. Sinauer  
 788 Associates, Sunderland, MA. pp. 423–442.  
 789 Ellison, J.C., 1989. Pollen analysis of mangrove sediments as a sea level  
 790 indicator: assessment from Tongatapu, Tonga. *Palaeogeography,*  
 791 *Palaeoclimatology, Palaeoecology* 74: 327–341.  
 792 Ellison, J.C., 2005. Holocene palynology and sea-level change in two estuaries in  
 793 Southern Irian Jaya. *Palaeogeography and Palaeoclimatology*. 220, 291–309.  
 794 Ellison, J.C., 2008. Long-term retrospection on mangrove development using  
 795 sediment cores and pollen analysis: A review. *Aquatic Botany* 89, 93–104.  
 796 Ellison, J.C., 2015. Vulnerability assessment of mangroves to climate change and  
 797 sea-level rise impacts. *Wetlands Ecology and Management*, 23(2), 115–137.  
 798 Engelhart, S.E., Horton, B.P., Roberts, D.H., Bryant, C.L., Corbett, D.R., 2007.  
 799 Mangrove pollen of Indonesia and its suitability as a sea level indicator. *Marine*  
 800 *Geology* 242, 65–81.  
 801 Fairbanks, R.G., 1989. A 17,000-year glacio-eustatic sea level record: influence of  
 802 glacial melting rates on the Younger Dryas event and deep- ocean circulation.  
 803 *Nature* 342, 639–642.

- 2281  
2282  
2283  
2284 804 Fisher, P. R., Dyer, K., Semesi, A. 1994. Rufiji Delta hydrodynamics research  
2285  
2286 805 program, Final report: Characteristic circulation and sedimentation in the Rufiji  
2287  
2288 806 delta, Tanzania. Frontier-Tanzania Technical report No. 13. The Society for  
2289  
2290 807 Environment Exploration. U.K.  
2291  
2292 808 Fleming, K., Johnston, P., Zwartz, D., Yokoyama, Y., Lambeck, K., Chappell, J.,  
2293  
2294 809 1998. Refining the eustatic sea-level curve since the Last Glacial Maximum using  
2295  
2296 810 far-and intermediate-field sites. Earth and Planetary Science Letters 163, 327–  
2297  
2298 811 342.  
2299  
2300 812 Francis, J. 1992. Physical processes in the Rufiji delta and their possible  
2301  
2302 813 implications on the mangrove ecosystem. Hydrobiologia 247, 173–179.  
2303  
2304 814 Gasse, F., 2000. Hydrological changes in the African tropics since the Last  
2305  
2306 815 Glacial Maximum. Quaternary Science Reviews 19, 189–211.  
2307  
2308 816 Gehrels, R., Long, A., 2008. Sea level is not level: the case for a new approach to  
2309  
2310 817 predicting UK sea-level rise. Geography 93(1), 11–16.  
2311  
2312 818 Gilman, E.L., Ellison, J., Duke, N.C. and Field, C., 2008. Threats to mangroves  
2313  
2314 819 from climate change and adaptation options: A review. Aquatic Botany 89(2),  
2315  
2316 820 237–250.  
2317  
2318 821 Goudie, A. S., 1996. Climate: past and present. In: Adams, W.A., Goudie, A.S.,  
2319  
2320 822 Orme, A.R. (eds) The physical geography of Africa. Oxford University Press,  
2321  
2322 823 New York, pp 34–59  
2323  
2324 824 Hait, A. K., Behling, H., 2009. Holocene mangrove and coastal environmental  
2325  
2326 825 changes in the western Ganga–Brahmaputra Delta, India. Vegetation History and  
2327  
2328 826 Archaeobotany 18, 159–169.  
2329  
2330 827 Hanebuth, T., Stattegger, K., Grootes, P.M., 2000. Rapid Flooding of the Sunda  
2331  
2332 828 Shelf: A Late-Glacial Sea-Level Record. Science 288, 1033–1035.  
2333  
2334  
2335  
2336  
2337  
2338  
2339  
2340



- 829 Hassan, F.A., 1997. Holocene Palaeoclimates of Africa. *African Archaeological*  
830 *Review* 14(4), 213–230.
- 831 Hijma, M., Engelhart, S.E., Törnqvist, T.E., Horton, B.P., Hu, P. and Hill, D.F.,  
832 2015. A protocol for a geological sea-level database. *Handbook of Sea-Level*  
833 *Research*, edited by: Shennan, I., Long, AJ, and Horton, BP, Wiley Blackwell, pp.  
834 536–553.
- 835 Horton, B.P., Benjamin, P., Gibbard, L.G., Milne, M., Morley, R.J.,  
836 Purintavaragul, C. and Stargardt, J.M., 2005. Holocene sea levels and  
837 palaeoenvironments, Malay-Thai Peninsula, Southeast Asia. *The Holocene* 15,  
838 1199–1213.
- 839 Isla, F.I., 1989. Holocene sea-level fluctuation in the Southern Hemisphere.  
840 *Quaternary Science Reviews* 8, 359–368.
- 841 Jaritz, W., Ruder, J., B, Schlenker, B., 1977. Das Quartar im Küstengebiet von  
842 Mocambique und seine Schwermineralführung. *Geologisches Jahrbuch, B*, 26: 3–  
843 93.
- 844 Katupotha, J., Fujiwara, K., 1988. Holocene sea level change on the southwest  
845 and south coasts of Sri Lanka. *Palaeogeography, Palaeoclimatology,*  
846 *Palaeoecology* 68, 189–203.
- 847 Kiage, L.M., Liu, K., 2006. Late Quaternary paleoenvironmental changes in East  
848 Africa: areview of multiproxy evidence from palynology, lake sediments, and  
849 associated records. *Progress in Physical Geography* 30 (5), 633–658.
- 850 Kibue, A. M., 2006. Sea level measurement and analysis in the Western Indian  
851 Ocean. National Report, Kenya.
- 852 Knopp, S., Mohammed, K.A., Simba Khamis, I., Mgeni, A.F., Stothard, J.R.,  
853 Rollinson, D., Marti, H., Utzinger, J., 2008. Spatial distribution of soil-transmitted

helminths, including *Strongyloides stercoralis*, among children in Zanzibar. Geospatial Health 3 (1), 47–56.

Lambeck, K., Nakada, M., 1990. Late Pleistocene and Holocene sea-level change along the Australian coast. Palaeogeography, Palaeoclimatology, Palaeoecology 89, 143–176.

Lambeck, K., Rouby, H., Purcell, A., Sun, Y., Sambridge, M., 2014. Sea level and global ice volumes from the Last Glacial Maximum to the Holocene. P Natl. Acad. Sci. U. S. A. 111, 15296–15303.

Larcombe, P., Carter, R.M., Dye, J., Gagan, M.K., Johnson, D.P., 1995. New evidence for episodic post-glacial sea-level rise, central Great Barrier Reef, Australia. Marine Geology 127, 1–44.

Lewis, S.E., Sloss, C.R., Murray-Wallace, C.V., Woodroffe, C.D. and Smithers, S.G., 2013. Post-glacial sea-level changes around the Australian margin: a review. Quaternary Science Reviews, 74, pp. 115–138.

Machiwa, J.F., Hallberg, R.O., 1995. Flora and crabs in a mangrove forest partly distorted by human activities. Zanzibar Ambio 24 (7–8), 492–496.

Mangora, M.M., Shalli, M.S., Semesi, I.S., Njana, M.A., Mwainunu, E.J., Otieno, J.E., Ntibasubile, E., Mallya, H.C., Mukama, K., Wambura, M. and Chamuya, N.A., 2016, January. Designing a mangrove research and demonstration forest in the rufiji delta, Tanzania. In Proceedings of the 5th Interagency Conference on Research in the Watersheds, pp. 190-192. US Department of Agriculture Forest Service, Southern Research Station.

Marchant, R.A., Hooghiemstra, H., 2004. Rapid environmental change in Africa and South American tropics around 4000 years before present. Earth Science Reviews 66, 217–260.

879 Masalu, D.C.P., 2003. Challenges of coastal area management in coastal  
880 developing countries—lessons from the proposed Rufiji Delta prawn farming  
881 project, Tanzania. *Ocean Coastal Management* 46, 175–188.

882 McCormac, F.G., Hogg, A.G., Blackwell, P.G., Buck, C.E., Higham, T.F.G.,  
883 Reimer, P.J., 2004. SHCal04 Southern Hemisphere Calibration, 0–11.0 cal kyr  
884 BP. *Radiocarbon* 46(3), 1087–1092.

885 McIvor, A.L., Spencer, T., Möller, I. and Spalding, M., 2013. The response of  
886 mangrove soil surface elevation to sea level rise. *Natural Coastal Protection*  
887 Series: Report 3. Cambridge Coastal Research Unit Working Paper 42. The  
888 Nature Conservancy and Wetlands International. 59 pp.

889 Milne, G., Long, A., Bassett, S., 2005. Modelling Holocene relative sea-level  
890 observations from the Caribbean and South America. *Quaternary Science*  
891 *Reviews* 24, 1183–1202.

892 Milne, G.A., Mitrovica, J.X., 2008. Searching for eustasy in deglacial sea-level  
893 histories. *Quaternary Science Reviews* 27, 2292–2302.

894 Mitrovica, J.X., Peltier, W.R., 1991. On postglacial geoid subsidence over the  
895 equatorial oceans. *Journal of Geophysical Research* 96, 20053–20071.

896 Mitrovica, J.X., Milne, G.A., 2002. On the origin of late Holocene sea-level  
897 highstands within equatorial ocean basins. *Quaternary Science Reviews* 21, 2179–  
898 2190.

899 Mörner, N., 1992. Ocean circulation, sea level changes and east African coastal  
900 settlements. In Sinclair, P.J.J., and Juma, A., (Eds.). *Urban Origins in Eastern*  
901 *Africa: Proceedings of the 1991 Workshop in Zanzibar*. Stockholm: Swedish  
902 Central Board of National Antiquities, pp. 256–266.

- 903 Mörner, N.A., 1996. Global change and interaction of earth rotation, ocean  
904 circulation and paleoclimate. *Anais da Academia Brasileira de Ciências*, 68, 77-  
905 94.
- 906 Mwandya, A.W., Gullstrom, M., Andersson, M.H., Ohman, M.C., Mgaya, Y.D.,  
907 Bryceson, I., 2010. Spatial and seasonal variations of fish assemblages in  
908 mangrove creek systems in Zanzibar (Tanzania). *Estuarine, Coastal and Shelf*  
909 *Science* 89(4), 277–286.
- 910 Nicholson, S.E., 2001. Climatic and environmental change in Africa during the  
911 last two centuries. *Climate research*, 17(2), 123-144.
- 912 Nshubemuki, L., 1993. Forestry resources in Tanzania's wetlands: concepts and  
913 potentials. *Wetlands of Tanzania*, 37–48.
- 914 Norström, E., Risberg, J., Gröndahl, H., Holmgren, K., Snowball, I., Mugabe, J.A.  
915 Siteo, S.R., 2012. Coastal Paleo-environment and Sea-level Change at Macassa  
916 Bay, Southern Mozambique, Since c 6600 Cal BP. *Quaternary International* 260,  
917 153–163.
- 918 Oerlemans, J., 2001. *Glaciers and climate change*. Library of Congress  
919 Cataloging-in-Publication Data.
- 920 Pirazzoli, P. A., Montaggioni, L. F., Salvat, B., & Faure, G., 1988. Late Holocene  
921 sea level indicators from twelve atolls in the central and eastern Tuamotus (Pacific  
922 Ocean). *Coral Reefs*, 7(2), 57–68.
- 923 Pirazzoli, P.A., 1991: *World Atlas of Holocene sea level changes*. Elsevier,  
924 Amsterdam, 300 pp.
- 925 Prendergast, M.E., Rouby, H., Punnwong, P., Marchant, R., Crowther, A.,  
926 Kourampas, N., Shipton, C., Walsh, M., Lambeck, K. and Boivin, N.L., 2016.

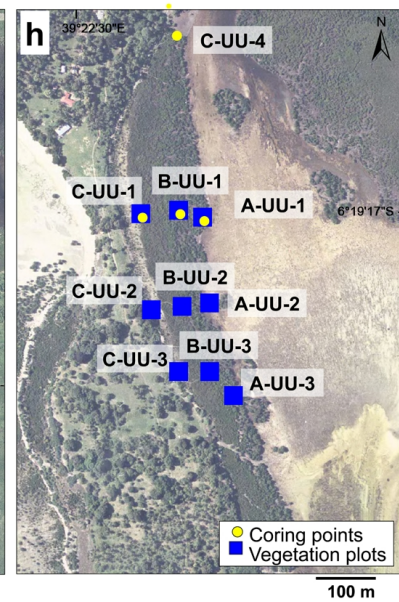
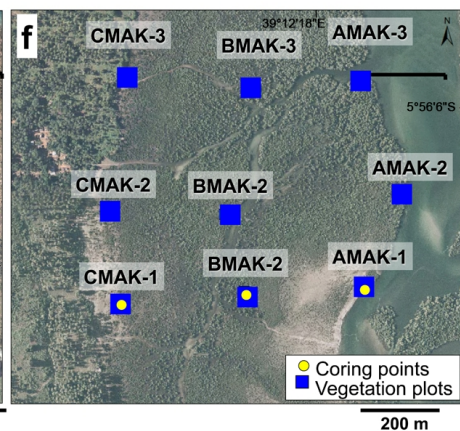
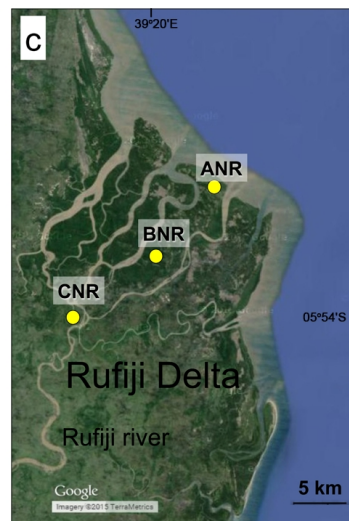
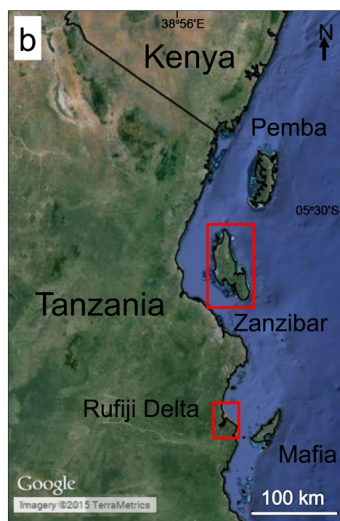
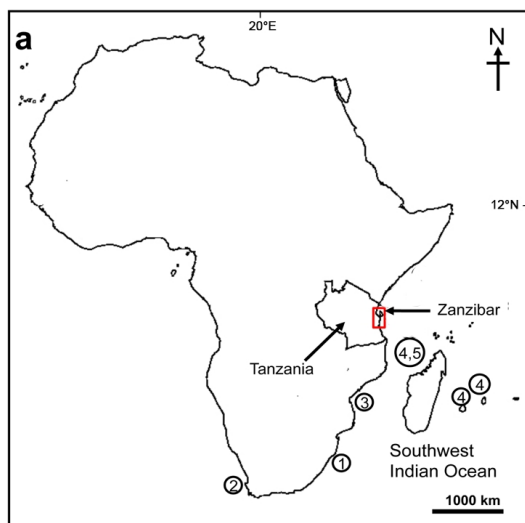
- 927 Continental island formation and the archaeology of defaunation on Zanzibar,  
928 eastern Africa. PLoS ONE 11(2): e0149565.
- 929 Punwong, P., Marchant, R., Selby, K., 2012. Holocene mangrove dynamics and  
930 environmental change in the Rufiji Delta, Tanzania. Vegetation History and  
931 Archaeobotany 22(5), 381–396.
- 932 Punwong, P., Marchant, R., Selby, K., 2013a. Holocene mangrove dynamics from  
933 Unguja Ukuu, Zanzibar. Quaternary International 298, 4–19.
- 934 Punwong, P., Marchant, R., Selby, K., 2013b. Holocene mangrove dynamics in  
935 Makoba Bay, Zanzibar. Palaeogeography Palaeoclimatology Palaeoecology 379–  
936 380, 54–67.
- 937 Ramsay, P.J., 1995. 9000 years of sea-level change along the southern African  
938 coastline. Quaternary International 31, 71–75.
- 939 Ramsay, P.J., Cooper, J. A. G., 2002. Late Quaternary Sea-Level Change in South  
940 Africa. Quaternary Research 57, 82–90.
- 941 Richmond, M. D., Wilson, J. D. K., Mgaya, Y. D., Le Vay, L. 2002. An analysis  
942 of smallholder opportunities in fisheries, coastal and related enterprises in the  
943 floodplain and delta areas of the Rufiji River, Tanzania. Rufiji Environment  
944 Management Project Technical report (25), 89 pp.
- 945 Rijdsdijk, K.F., Zinke, J., de Loux, P.G.B., Hume, J.P., van der Plicht, H.,  
946 Hooghiemstra, H., Meijer, H.J.M., Vonhof, H., Porch, N., Florens, V., Baider, C.,  
947 van Geel, B., Brinkkemper, J., Vernimmen, T., Janoo, A., 2011. Mid-Holocene  
948 (4200 kyr BP) mass mortalities in Mauritius (Mascarenes): Insular vertebrates  
949 resilient to climatic extremes but vulnerable to human impact. The Holocene, 1–  
950 16.

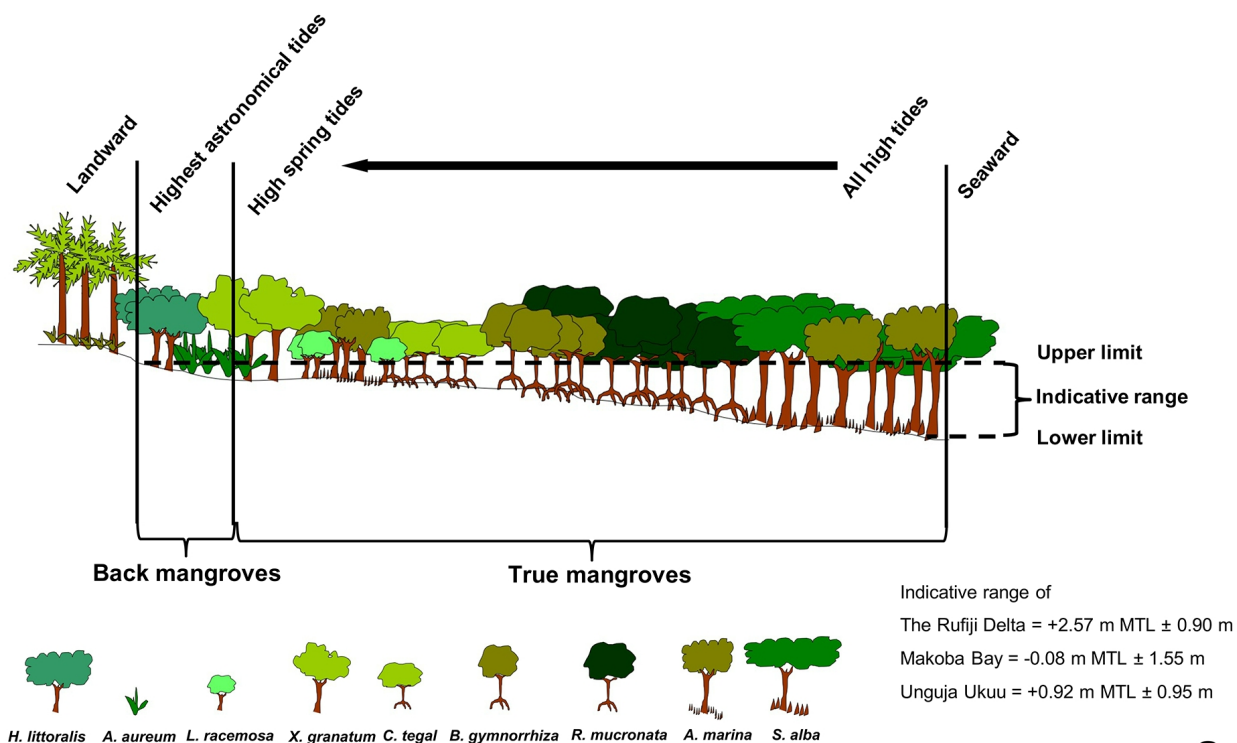
- 951 Santisuk, T., 1983. Taxonomy and distribution of terrestrial trees and shrubs in  
952 the mangrove formations in Thailand. The Natural History Bulletin of the Siam  
953 Society. 5 (1), 63–91.
- 954 Schlüter, T., 1997. Geology of East Africa. Gebrüder Borntraeger, Berlin, 484 pp.
- 955 Semesi, A. K., 1992. The mangrove resource of the Rufiji delta, Tanzania. In:  
956 Matiza T, Chabwela HN (Eds.) Wetlands conservation conference for southern  
957 Africa. Proceedings of the southern African development coordination conference  
958 held in Gaborono, Botswana, 3–5 June 1991. Union Internationale pour la  
959 Conservation de la Nature et de ses Ressources, Switzerland (UICN), Gland, pp  
960 157–172.
- 961 Shennan, I., Innes, J. B., Long, A. J., & Zong, Y. 1995. Late Devensian and  
962 Holocene relative sea-level changes in northwestern Scotland: new data to test  
963 existing models. Quaternary International, 26, 97–123.
- 964 Shunula, J.P., 2002. Public awareness, key to mangrove management and  
965 conservation: the case of Zanzibar. Trees 16, 209–212.
- 966 Sloss, C. R., Murray-Wallace, C. V., & Jones, B. G., 2007. Holocene sea-level  
967 change on the southeast coast of Australia: a review. The Holocene, 17(7), 999–  
968 1014.
- 969 Stocker, T.F., Qin, D., Plattner, G.K., Tignor, M., Allen, S.K., Boschung, J.,  
970 Nauels, A., Xia, Y., Bex, B. and Midgley, B.M., 2013. IPCC, 2013: climate  
971 change 2013: the physical science basis. Contribution of working group I to the  
972 fifth assessment report of the intergovernmental panel on climate change.
- 973 Thompson, L.G., Mosley-Thompson, E., Davis, M.E., Henderson, K.A., Brecher,  
974 H.H., Zagorodnov, V.S., Mashiotto, T.A., Lin, P., Mikhaleiko, V.N., Hardy,

- 975 D.R., Beer, J., 2002. Kilimanjaro ice core records: evidence of Holocene climate  
976 change in tropical Africa. *Science* 298, 589–593.
- 977 Tossou, M.G., Akoègninoua, A., Balloucheb, A., Sowunmic, M.A., Akpagana,  
978 K., 2008. The history of the mangrove vegetation in Bénin during the Holocene:  
979 A palynological study. *Journal of African Earth Sciences* 52, 167–174.
- 980 Vedel, V., Behling, H., Cohen, M., Lara, R., 2006. Holocene mangrove dynamics  
981 and sea-level changes in northern Brazil, inferences from the Taperebal core in  
982 northeastern Pará State. *Vegetation History and Archaeobotany* 15, 115–123.
- 983 Verschuren, D., Laird, K.R. and Cumming, B.F., 2000. Rainfall and drought in  
984 equatorial east Africa during the past 1,100 years. *Nature*, 403(6768), 410–414.
- 985 Watson, J. G. 1928. Mangrove forests of the Malay Peninsula. *Malayan Forest*  
986 *Records* 6, 275 pp.
- 987 Woodroffe, C.D., Grindrod, J., 1991. Mangrove Biogeography: The Role of  
988 Quaternary Environmental and Sea-Level Change. *Journal of Biogeography* 18,  
989 479.
- 990 Woodroffe, S.A., Horton, BP, 2005. Holocene sea-level changes in the Indo-  
991 Pacific. *Journal of Asian Earth Sciences* 25, 29–43.
- 992 Woodroffe, S.A., 2006. Holocene relative sea-level changes in Cleveland Bay,  
993 North Queensland, Australia. PhD thesis, University of Durham, 155 pp.
- 994 Woodroffe, S. A., Long, A.J., Punwong, P., Selby, K., Bryant, C.L., Marchant, R.,  
995 2015a. Radiocarbon dating of mangrove sediments to constrain Holocene sea-  
996 level change on Zanzibar in the Southwest Indian Ocean. *The Holocene* 25(5),  
997 820–831.

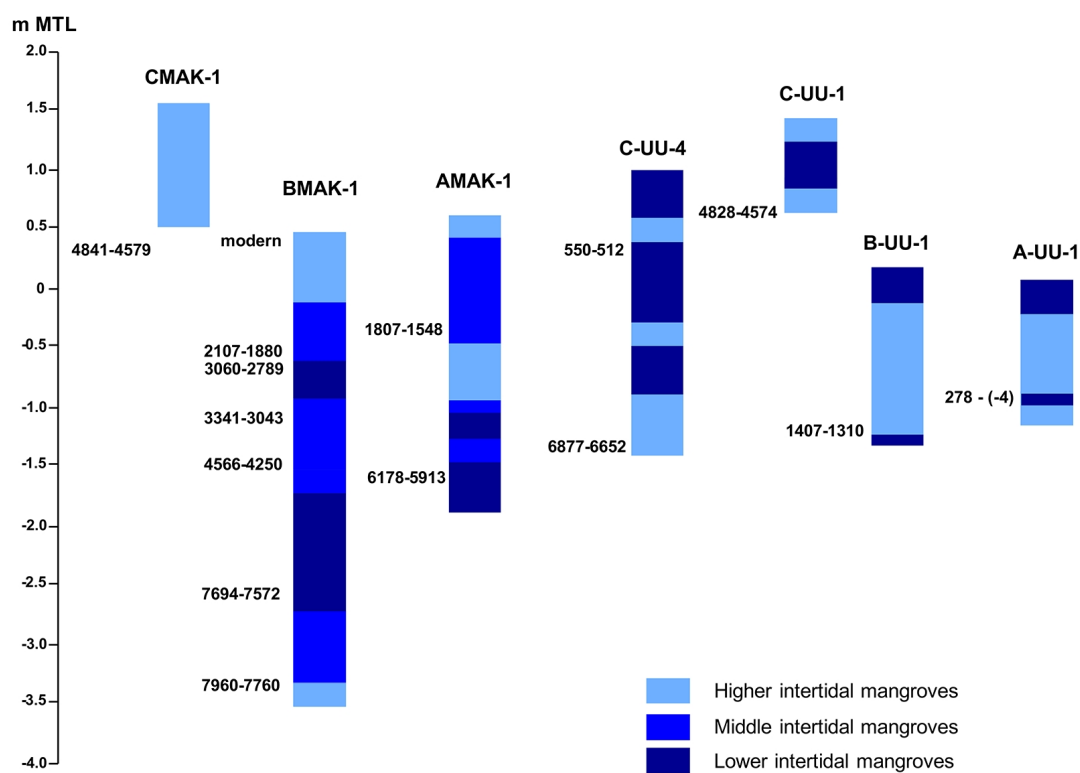
- 2761  
2762  
2763  
2764 998 Woodroffe, S. A., Long, A. J., Milne, G. A., Bryant, C. L., & Thomas, A. L.  
2765  
2766 999 2015b. New constraints on late Holocene eustatic sea-level changes from Mahé,  
2767  
2768 1000 Seychelles. *Quaternary Science Reviews* 115, 1–16.  
2769  
2770 1001 Zinke, J., Reijmer, J.J.G., Dullo, W. C., Thomassin, B.A., 2000.  
2771  
2772 1002 Paleoenvironmental changes in the lagoon of Mayotte associated with the  
2773  
2774 1003 Holocene transgression. *Geolines* 11, 150–153.  
2775  
2776 1004 Zinke, J., Reijmer, J.J.G., Thomassin, B.A., Dullo, W. C., Grootes, P.M. and  
2777  
2778 1005 Erienkeuser, H., 2003. Postglacial flooding history of Mayotte Lagoon (Comoro  
2779  
2780 1006 Archipelago, southwest Indian Ocean). *Marine Geology*, 194 (3-4), 181–196.  
2781  
2782  
2783  
2784  
2785  
2786  
2787  
2788  
2789  
2790  
2791  
2792  
2793  
2794  
2795  
2796  
2797  
2798  
2799  
2800  
2801  
2802  
2803  
2804  
2805  
2806  
2807  
2808  
2809  
2810  
2811  
2812  
2813  
2814  
2815  
2816  
2817  
2818  
2819  
2820



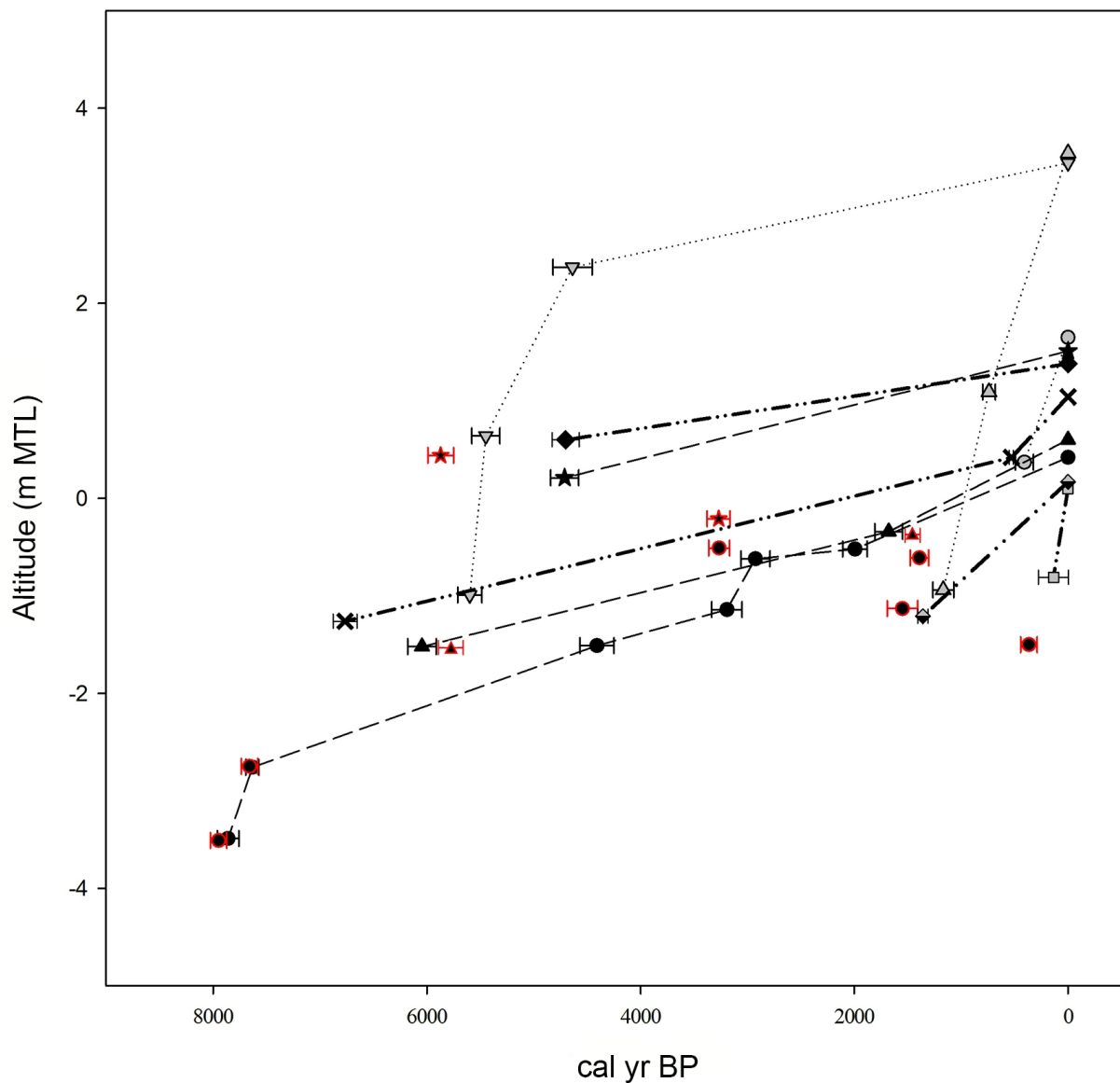




a



b



#### The Rufiji Delta

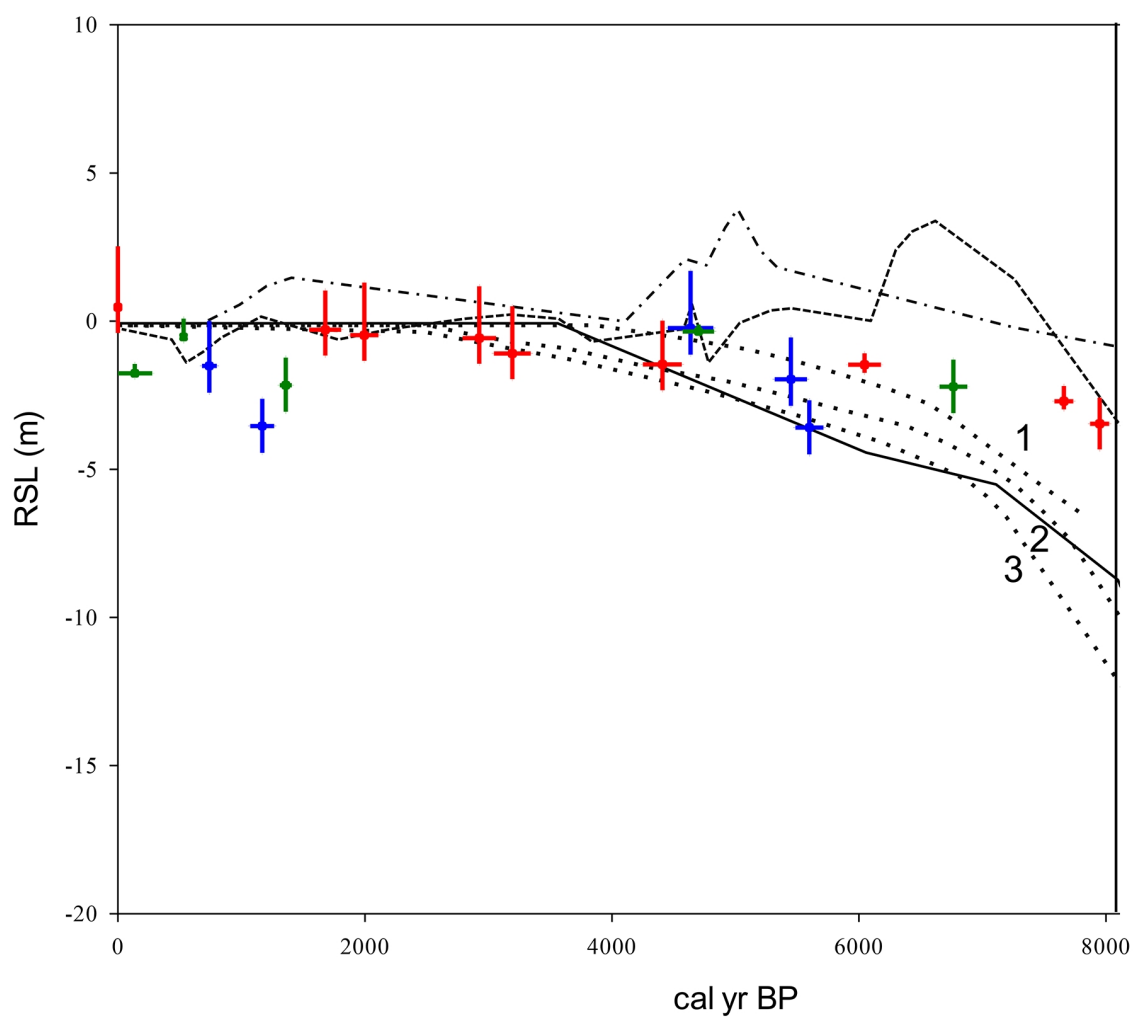
.....○..... ANR  
 .....▽..... BNR  
 .....△..... CNR

#### Makoba Bay

---▲--- AMAK-1  
 ---●--- BMAK-1  
 ---★--- CMAK-1

#### Unguja Ukuu

---□--- A-UU-1  
 ---◇--- B-UU-1  
 ---◆--- C-UU-1  
 ---×--- C-UU-4



— RSL from The northern Rufiji Delta  
 — RSL from Makoba Bay  
 — RSL from Unguja Ukuu

- - - RSL from Compton (2001)  
 - . - RSL from Ramsay and Cooper (2002)  
 . . . RSL from Camoin et al. (1997; 2004)  
 (1) Mauritius, (2) Mayotte, (3) Réunion  
 — RSL from Zinke *et al.* (2003)